6-18-2021

# The sensitivity of Neotoma to climate change and biodiversity loss over the late Quaternary

Catalina P. Tomé
*University of Nebraska-Lincoln*, ctome2@unl.edu

S. Kathleen Lyons
*University of Nebraska - Lincoln*, katelyons@unl.edu

Seth D. Newsome
*University of New Mexico*, newsome@unm.edu

Felisa A. Smith
*University of New Mexico*, fasmith@unm.edu

# The sensitivity of Neotoma to climate change and biodiversity loss over the late Quaternary

Catalina P. Tomé,[1,2] S. Kathleen Lyons,[1]
Seth D. Newsome,[2] and Felisa A. Smith [2]

1 School of Biological Sciences, University of Nebraska-Lincoln, NE 68588
2 Department of Biology, University of New Mexico, Albuquerque, NM 87131

*Corresponding author* — C.P. Tomé, email ctome2@unl.edu

**Abstract**

The late Quaternary in North America was marked by highly variable climate and considerable biodiversity loss including a megafaunal extinction event at the terminal Pleistocene. Here, we focus on changes in body size and diet in *Neotoma* (woodrats) in response to these ecological perturbations using the fossil record from the Edwards Plateau (Texas) across the past 20,000 years. Body mass was estimated using measurements of fossil teeth and diet was quantified using stable isotope analysis of carbon and nitrogen from fossil bone collagen. Prior to ca. 7,000 cal yr BP, maximum mass was positively correlated to precipitation and negatively correlated to temperature. Independently, mass was negatively correlated to community composition, becoming more similar to modern over time. *Neotoma* diet in the Pleistocene was primarily sourced from $C_3$ plants, but became progressively more reliant on $C_4$ (and potentially CAM) plants through the Holocene. Decreasing population mass and higher $C_4$/CAM consumption was associated

Published in *Quaternary Research* 105 (2021), pp. 49-63.
doi:10.1017/qua.2021.29

Submitted 29 June 2020; accepted 19 April 2021; published 18 June 2021.

with a transition from a mesic to xeric landscape. Our results suggest that *Neotoma* responded to climatic variability during the terminal Pleistocene through changes in body size, while changes in resource availability during the Holocene likely led to shifts in the relative abundance of different *Neotoma* species in the community.

**Keywords:** megafaunal extinction, small mammal response, Edwards Plateau

## Introduction

The terminal Pleistocene (20,000–11,700 cal yr BP) encompassed a period of substantial restructuring of North American terrestrial ecosystems, which were linked to the combined effects of changing climate and substantial biodiversity loss (e.g., Barnosky et al., 2016; Cotton et al., 2016; Smith et al., 2016b; Tóth et al., 2019). As glaciers retreated to the north after the last glacial maximum at 21,000 cal yr BP, climate warmed by ~8°C overall, although this warming was interrupted by numerous temperature reversals (Cole and Arundel, 2005; IPCC, 2014). The most notable of these was the Younger Dryas (12,800–11,500 cal yr BP), a 1,300 year period of cooling to near glacial conditions, which ended in a particularly rapid 5–7°C increase in temperature over a few decades (Dansgaard, 1989; Alley, 2000). These environmental fluctuations influenced the composition and distribution of flora and fauna across North America (Prentice et al., 1991; Graham et al., 1996; Grayson, 2000; Lyons, 2003, 2005; Blois et al., 2010; Cotton et al., 2016).

The terminal Pleistocene was also unique because within a few hundred years, virtually all large-bodied mammals (>150 species) went extinct in the Americas (Martin, 1967; Martin and Klein, 1989; Martin and Steadman, 1999; Lyons et al., 2004). Highly size-selective, this event saw the loss of all mammals weighing >600 kg—a diverse group of megafauna including mammoths, camels, and giant ground sloths (Lyons et al., 2004; Smith et al., 2018). Large-bodied mammals have substantial impacts within modern communities and ecosystems, both through environmental engineering and species interactions (Janzen and Martin, 1982; Owen-Smith, 1992; Ripple et al., 2015; Malhi et al., 2016; Smith et al., 2016a). For example, extant megaherbivores in

Africa help maintain savanna and grassland habitats by suppressing woody growth, modifying fire regimes, and acting as seed dispersers for plants (Dublin et al., 1990; Owen-Smith, 1992; Goheen et al., 2010, 2018). Exclusion of these large-bodied mammals can result in shifts in vegetation composition and abundance and/or alter the distribution and abundance of other mammals, such as rodents, via competitive interactions (Keesing, 1998; Goheen et al., 2004, 2018; Parsons et al., 2013; Keesing and Young, 2014; Koerner et al., 2014; Galetti et al., 2015). Pleistocene megafauna are thought to have played roles similar to their modern counterparts by maintaining open habitats and enhancing species diversity, repressing fire regimes, and increasing nutrient availability across ecosystems (Johnson, 2009; Rule et al., 2012; Doughty et al., 2013; Ripple et al., 2015; Bakker et al., 2016). In addition to structural changes in vegetation, the extinction likely had cascading effects on community structure and interactions of the surviving mammal species (Smith et al., 2016b; Tóth et al., 2019).

How these wholesale changes in community dynamics and climate influenced surviving species likely depended on whether species were more sensitive to abiotic or biotic interactions. Changes in temperature often lead to shifts in body size, diet, or both, either as a direct consequence of thermal physiology or due to shifting vegetation composition (Bergmann, 1847; Brown, 1968; Andrewartha and Birch, 1986; Brown and Heske, 1990; Smith et al., 1995; Ashton et al., 2000; Stenseth et al., 2002; Millien et al., 2006; Walsh et al., 2016). Because body size scales with most life history traits and physiological processes, including metabolism, ingestion, and thermal regulation (McNab, 1980; Peters, 1983; Justice and Smith, 1992; Smith, 1995a), size can influence the types and amounts of resources available to consumers, as well as inter- and intraspecies interactions among consumers (Damuth, 1981; Peters, 1983). At a local scale, enhanced competition for habitat and resources will decrease the abundances of species of similar size that share resources (Brown, 1973; M'Closkey, 1976; Bowers and Brown, 1982; Brown and Nicoletto, 1991; Auffray et al., 2009). The relationship between body size and other ecological factors (such as home range or competition), particularly when combined with dietary and environmental information, can be used to quantify complex ecosystem and community changes recorded in the paleontological record (Damuth, 1981).

Here, we characterize the response of *Neotoma* (woodrats) to environmental and ecological perturbations on the Edwards Plateau (Texas) (**Figure 1**A–B) over the past ca. 22,000 years. We quantify shifts in body size and diet using digital imaging of fossil molars and stable isotope analysis of associated bone collagen, respectively. We focus on a complex of three potential *Neotoma* species—*N. albigula* (white-throated woodrat), *N. floridana* (eastern woodrat), and *N. micropus* (southern plains woodrat)—which differ in body size, dietary preferences, and habitat affinity. All species of *Neotoma* are herbivorous and construct large dens. *Neotoma albigula* (~155–250 g) and *N. micropus* (~180–320 g) both inhabit desert and semi-arid environments and are reliant on cacti for den construction and as a source of food and water (Olsen, 1976; Macêdo and Mares, 1988; Braun and Mares, 1989; Orr et al., 2015). In contrast, *N. floridana* (~200–380 g) typically inhabit more mesic, forested environments, do not usually forage on cacti, and typically eat higher proportions of leaves and fruit from trees and shrubs (Rainey, 1956; Finley, 1958; Wiley, 1980). Woodrat dens are typically built within rock crevices, which provide protection from both predators and extreme temperatures (Finley, 1958; Brown, 1968; Brown et al., 1972; Smith, 1995b; Murray and Smith, 2012). Past studies of *Neotoma* suggest all species within the genus are highly sensitive to temperature; morphological changes in size are a common response to temperature fluctuations across both space and time (Brown and Lee, 1969; Smith et al., 1995, 1998; Smith and Betancourt, 1998, 2003). These changes in size align with the ecological principle known as Bergmann's Rule—the idea that within a genus, those species inhabiting colder environments will be larger than those in warmer ones (Bergmann, 1847; Mayr, 1956; Brown and Lee, 1969; Ashton et al., 2000; Freckleton et al., 2003; Smith, 2008). Thus, we hypothesize that *Neotoma* species were strongly influenced by temperature fluctuations on the Edwards Plateau, with increasing Holocene temperatures leading to a decrease in body mass.

Changes in vegetation associated with climate and the terminal Pleistocene megafaunal extinction may have also led to shifts in resource availability and competition among consumers that are reflected in shifts in diet composition among sympatric species. Body mass is an important component of interspecific interactions for

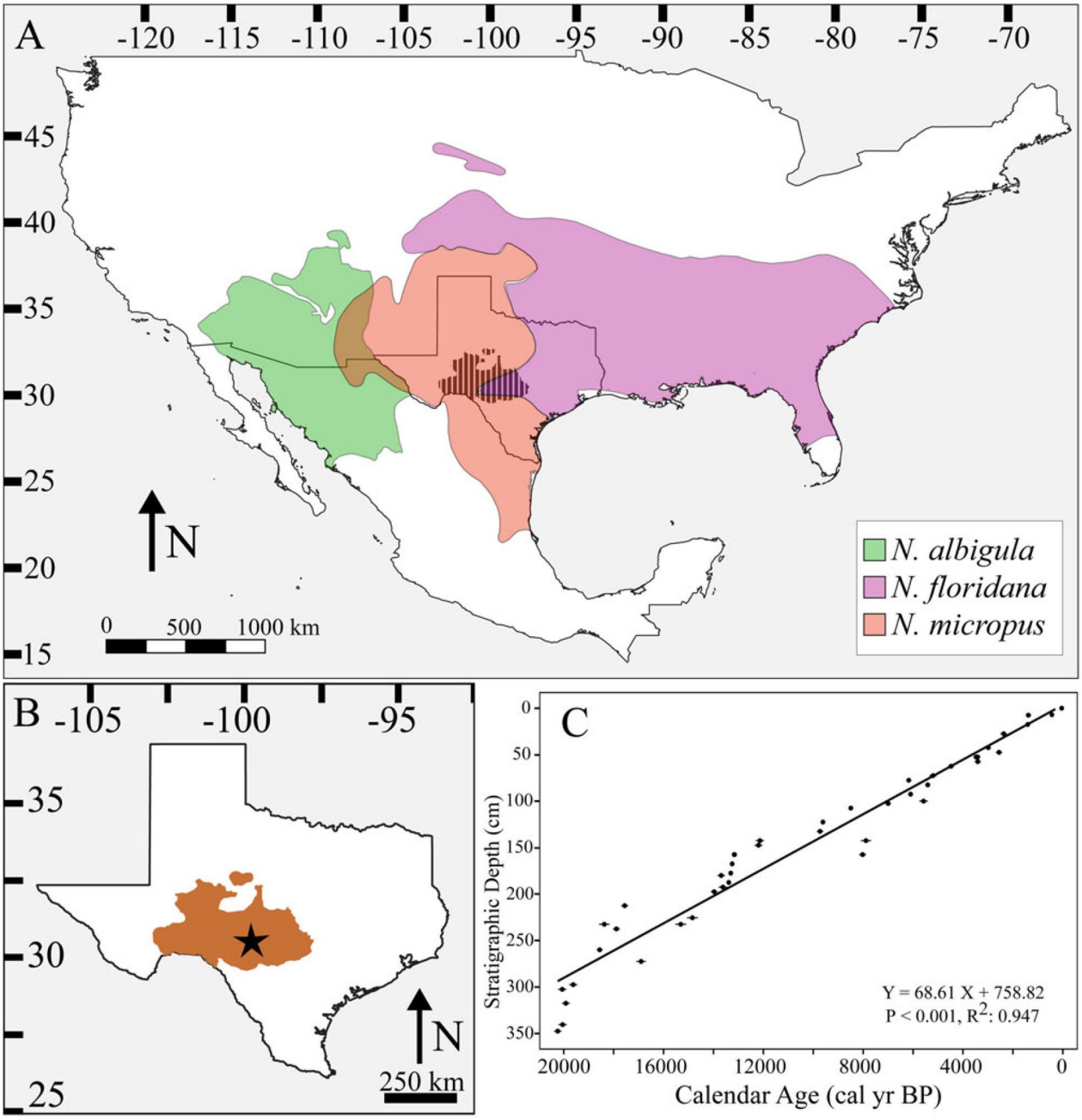


**Figure 1.** Neotoma species distributions. (A) Map of North America with modern distributions of *Neotoma albigula* (green), *N. floridana* (purple), and *N. micropus* (red). Location of the Edwards Plateau in Texas is represented by cross-hatched black area. (B) Map of Texas with Edwards Plateau highlighted in brown and location of Hall's Cave (star). (C) The age model, which is composed of 44 AMS $^{14}$C measurements previously combined from Toomey (1993), Cooke et al. (2003), and Bourne et al. (2016) and calibrated by Tomé et al. (2020a).

*Neotoma*. When different species of *Neotoma* occur in sympatry, the smaller-bodied species may shift microhabitats or diet to partition resources with larger-bodied ones (Finley, 1958; Cameron, 1971; Dial, 1988). For example, where they co-occur with larger *N. fuscipes* (~230–300 g), *N. lepida* (~120–240 g) switch from feeding on oaks (*Quercus turbinella*) to feeding on juniper (*Juniperus californica*); consumption of juniper has a higher metabolic and thermoregulatory cost for woodrats because it contains higher concentrations of toxic secondary compounds (Cameron, 1971; Carraway and Verts, 1991; Verts and Carraway, 2002; McLister et al., 2004; Dearing et al., 2005). Community reorganization following the extinction thus may have influenced dietary responses in *Neotoma* either though changes in competition for available resources or through shifts in the relative abundance of vegetation driven by the absence of megaherbivores.

We assessed dietary changes over time with carbon ($\delta^{13}C$) and nitrogen ($\delta^{15}N$) isotope analyses of bone collagen, which have previously been used to quantify changes in diet composition, trophic level, and niche partitioning across space and time (Chamberlain et al., 2005; West et al., 2006; Koch et al., 2009; Leonard et al., 2007; Smiley et al., 2016). Changes in diet and body size may also reflect species preferences in terms of environmental conditions and resource availability. During the last glacial maximum (ca. 21,000 cal yr BP), the Edwards Plateau was a mix of deciduous forest and conifers, before warming and drying conditions during the late-glacial period (17,000–11,600 cal yr BP) led to the transition to a grassland and oak savanna landscape (Bryant and Holloway, 1985; Cordova and Johnson, 2019). This vegetation remained relatively stable throughout the Holocene (11,600–0 cal yr BP), and today the region is predominantly a savanna shrub woodland populated by oak, mesquite, and juniper (Bryant and Holloway, 1985; Toomey et al., 1993; Joines, 2011). As regional vegetation shifted from mesic conditions preferred by *N. floridana* to a drier shrubland more preferred by *N. albigula* and *N. micropus*, we may expect to see shifts in diet towards resources more typically used by arid-adapted woodrats (e.g., higher consumption of cacti) due either to changes in resource use or changes in the relative abundance of these three species over time.

## Methods

### *Study site*

We used fossils from Hall's Cave in the Edwards Plateau, Texas (Figure1B). This site is a fluvial deposit with episodic deposition of sediments and biological materials following heightened periods of precipitation (Toomey, 1993). The Hall's Cave record extends back to ca. 20,000 cal yr BP, with an exceptionally well-dated stratigraphic sequence (Figure1C). Excavations from Hall's Cave began in the 1960s and accelerated in the late 1980s– 1990s (Toomey, 1993). To date, the site has yielded thousands of vertebrate specimens, particularly of small and medium body sizes across various trophic guilds (Toomey, 1993). The vertebrate fossils are housed at the Vertebrate Paleontology Lab of the Texas Memorial Museum (TMM) at the University of Texas, Austin.

### *Study organisms*

Three *Neotoma* species are hypothesized to be present in the Hall's Cave fossil record: *N. albigula*, *N. floridana*, and *N. micropus* (Toomey, 1993), with the latter two extant on the Edward's Plateau today (Figure1A). Unfortunately, the three species cannot be distinguished based solely on molar or lower-jaw characteristics (Sagebiel, 2010; Tomé et al., 2020b), which represent the vast majority of our fossil elements. Moreover, there is substantial body size overlap among the species. Thus, we aggregated samples and asked questions at the level of the genus, which we note is common for paleoecological studies. Nonetheless, we note that preliminary ancient DNA work conducted on a sediment column taken from Hall's Cave suggested a high probability that *Neotoma floridana* is the only woodrat present in the oldest (prior to the extinction boundary at ca. 13,000 cal yr BP) stratigraphic levels (Seersholm et al., 2020).

*Neotoma* fossils are present in all strata at Hall's Cave from ca. 22,000 cal yr BP to modern deposits (Toomey, 1993); however, specimen abundance varies by stratum. To facilitate our analyses of body size and diet of *Neotoma* over time, we aggregated data into 15 time intervals of approximately equal length, chosen and accounting for important environmental transitions (**Table 1**). Note that the oldest time

**Table 1.** Summary of data for Neotoma by time interval. Precipitation, maximum and minimum temperature were extracted from the CCM3 (Lorenz et al., 2016a, b) in 500 year intervals and average each time interval given below. Sorenson to Modern is the Sorenson Index calculated in terms of similarity to the community composition of the youngest time interval (0–1500 cal BP).

| *Age Range (cal yr BP)* | *N Mass* | *N Isotopes* | *Mean Mass (g) (±SD)* | *Mean $\delta^{13}C$ (±SD)* | *Mean $\delta^{15}N$ (±SD)* | *% C3 in Diet (%)* | *Maximum Temperature (°C) (±SD)* | *Minimum Temperature (°C) (±SD)* | *Mean Precipitation (mm) (±CV)* | *Species Richness* | *Similarity to Modern* | *Turnover* |
|---|---|---|---|---|---|---|---|---|---|---|---|---|
| 1,500–0 | 10 | 9 | 170.4±32.0 | −17.8±3.1 | 5.9±1.3 | 48.3±13.5 | 25.5±7.1 | 12.1±7.4 | 554.6±0.4 | 35 | 1.00 | 0.97 |
| 3,100–1,500 | 35 | 14 | 186.2±30.2 | −19.4±1.8 | 5.7±1.5 | 59.0±8.0 | 25.5±7.2 | 11.8±7.6 | 534.7±0.4 | 37 | 0.97 | 0.85 |
| 5,400–3,100 | 63 | 49 | 209.4±50.3 | −17.8±2.5 | 5.8±1.1 | 48.0±9.0 | 25.4±7.8 | 11.8±7.6 | 558.4±0.4 | 34 | 0.84 | 0.88 |
| 6,100–5,400 | 27 | 20 | 204.9±48.4 | −17.8±2.3 | 5.4±1.3 | 47.9±9.3 | 25.3±8.0 | 11.9±7.9 | 553.1±0.4 | 30 | 0.83 | 0.89 |
| 6,400–6,100 | 16 | 9 | 197.6±42.9 | −17.6±1.9 | 5.8±1.0 | 47.0±9.9 | 25.5±8.1 | 11.8±8.1 | 536.3±0.4 | 33 | 0.85 | 1.00 |
| 6,700–6,400 | 12 | 11 | 192.0±52.0 | −18.6±2.0 | 5.2±1.7 | 53.7±9.5 | 25.5±8.2 | 11.9±8.2 | 526.8±0.4 | 33 | 0.85 | 1.00 |
| 7,700–6,700 | 32 | 32 | 189.2±37.1 | −16.9±2.8 | 5.9±1.1 | 41.5±9.9 | 25.1±8.7 | 11.9±8.3 | 536.7±0.4 | 33 | 0.85 | 1.00 |
| 8,400–7,700 | 17 | 22 | 210.0±41.6 | −18.2±1.8 | 5.8±0.9 | 50.6±7.7 | 25.0±9.0 | 11.9±8.4 | 532.0±0.4 | 33 | 0.85 | 0.91 |
| 9,000–8,400 | 23 | 22 | 209.0±42.2 | −17.5±2.1 | 6.5±1.3 | 45.6±8.1 | 24.8±9.2 | 11.9±8.6 | 539.1±0.3 | 37 | 0.78 | 1.00 |
| 9,400–9,000 | 10 | 9 | 221.3±48.9 | −18.2±2.6 | 6.4±1.7 | 50.5±12.2 | 24.9±9.2 | 11.9±8.7 | 552.5±0.3 | 37 | 0.78 | 0.82 |
| 10,000–9,400 | 21 | 20 | 219.8±43.9 | −17.8±2.8 | 6.2±1.2 | 47.6±10.6 | 24.8±9.3 | 11.8±8.6 | 561.5±0.3 | 46 | 0.74 | 1.00 |
| 11,000–10,000 | 32 | 34 | 216.7±48.7 | −19.4±1.2 | 5.9±1.2 | 58.9±5.3 | 24.3±9.2 | 11.5±8.7 | 582.4±0.3 | 46 | 0.74 | 0.80 |
| 12,700–11,000 | 53 | 21 | 205.5±43.2 | −19.2±1.0 | 6.0±1.5 | 57.7±4.2 | 22.9±9.7 | 10.7±9.0 | 628.1±0.3 | 59 | 0.60 | 0.83 |
| 15,800–12,700 | 56 | 29 | 210.3±52.4 | −18.9±1.6 | 5.0±1.5 | 55.7±7.2 | 22.1±10.1 | 10.0±9.5 | 631.0±0.3 | 71 | 0.51 | 0.85 |
| 22,400–15,800 | 23 | 5 | 226.9±54.2 | −19.5±0.3 | 4.2±1.1 | 59.8±2.6 | 18.7±10.4 | 7.1±10.2 | 685.9±0.4 | 65 | 0.40 | |

interval is longer, spanning 22,400–15,800 cal yr BP; this is because *Neotoma* fossil bones were rare, with only 31 elements recovered in this interval. Thus, to increase sample size, we also included a sample of 14 additional *Neotoma* specimens from Zesch Cave, a nearby fossil site, ~75 km away, at 470 m in elevation, and dating to 18,000– 16,000 cal yr BP (Lundelius, 1967; Graham et al., 1987; Sagebiel, 2010). The Zesch Cave record shares a similar community composition to that of Hall's Cave, including the same three potential *Neotoma* species. To verify that climatic regimes at this time were similar between Zesch Cave and Hall's Cave (~680m elevation), we compared climate data from the Community Climate System Model (Lorenz et al., 2016a, b). We found that mean annual precipitation, maximum temperature, and minimum temperature differed by ~32.5 mm, ~7.1°C, and 4.7°C, respectively, between the two sites, with temperature differences falling within one standard deviation for the time bin spanning 22,400–15,800 cal yr BP. Two sample t-tests found no significant difference in body size or bone collagen $\delta^{13}C$ and $\delta^{15}N$ values of *Neotoma* from Zesch Cave and Hall's Cave (Supplementary Table S1). All other (i.e., younger) time bins include only specimens from Hall's Cave.

### *Morphology*

We estimated body size in *Neotoma* using linear measurements of the first upper (UM1) and lower molars (LM1). These molars were either loose or found in mandibular or maxillary elements, generally with incomplete toothrows. The upper or lower M1 of 693 *Neotoma* fossils were photographed using a calibrated AM4515ZT Dino-Lite Edge digital microscope. The length of each molar was measured three times (~2080 measurements) using the line tool in DinoCapture 2.0. Samples that could not be well characterized or whose measurements resulted in a >5% standard error were discarded, which led to the elimination of 22 specimens. We calculated the minimum number of individuals (MNI) to exclude potentially replicated individuals because it was not possible to determine whether loose molars were definitively from different specimens or potentially from different quadrants (upper right and left, and lower right and left) from the same individual.

To help in the estimation of MNI, we determined the 'normal' asymmetry of teeth found among modern woodrats. By measuring all the first molars (upper and lower, right and left) for a total of 20 museum specimens, which included individuals from the species *Neotoma floridana* and *N. albigula* from the Museum of Southwestern Biology (MSB) at the University

of New Mexico (Albuquerque, NM) and the James F. Bell Museum of Natural History (MMNH) at the University of Minnesota (St. Paul, MN) (Supplementary Table S2), we characterized the upper versus lower and bilateral symmetry of woodrat teeth. We found that on average, upper first molars (UM1) were ~5% larger than lower first molars (LM1). Moreover, bilateral symmetry was high, with only an average difference of ~0.5% between left and right measurements. These results were independent of species and provided a strategy for analysis: using 0.5% as a cutoff we were able to determine whether loose molars from a stratum could realistically belong to different *Neotoma*. First, we preferentially selected only lower left first molars (LLM1s) for each stratigraphic level. Second, we then included all lower right first molars (LRM1s) from that level that were 0.5% greater or smaller in size than any measured LLM1s in the sample. Third, after standardizing the size of upper molars to that of lower molars with a 5% length reduction, we included upper left first molars (ULM1s) from that level that were 0.5% greater or smaller in size than any lower molars selected in the first two steps. Lastly, we included upper right first molars (URM1s) from the same level that were 0.5% greater or smaller in size than any previously selected LLM1s, LRM1s, and ULM1s. Thus, we ensured that separately measured elements were not from the same individual within a stratum.

Tooth measurements were translated into estimates of body mass using an allometric equation for cricetid rodents for the first lower molar length (Martin, 1990):

$$\text{Log mass (g)} = 3.310 * (\text{Log LM1 length}) + 0.611$$

$$(r^2 = 0.96, \%PE = 15.58, df = 32)$$

To account for differences between lower and upper molar length in *Neotoma*, upper molar length was standardized by a 5% decrease to measurements prior to calculating body mass. After the removal of potential duplicates, our final dataset included body mass estimates for 430 individual *Neotoma* across the 15 levels, including mass estimates for 10–63 individuals per time bin (Table 1).

### *Isotope-based estimates of diet composition and variation*

We used stable isotope analysis to characterize shifts in diet for *Neotoma* across time. We measured carbon ($\delta^{13}C$) and nitrogen ($\delta^{15}N$) isotope values of bone collagen extracted from maxillary and mandible bones for 367 *Neotoma* fossils. We attempted to acquire 10 or more samples per time interval; however, sparsity of material led to some intervals containing fewer than 10 individuals, and we excluded a single interval that only contained five

individuals (22,400–15,800 cal yr BP). Differences in how plants that use the $C_3$ versus $C_4$ photosynthetic pathway fractionate carbon isotopes leads to natural variation in $\delta^{13}C$ values across ecosystems and are reflected in the tissues of consumers that utilize these resources (DeNiro and Epstein, 1978; Farquhar et al., 1989; Cerling et al., 1997). Regional studies in the Great Plains and southern/central Texas have found that $C_3$ and $C_4$ plants have mean (±SD) $\delta^{13}C$ values of about −27 ± 5‰ and −13 ± 4‰, respectively (Boutton et al., 1993, 1998; Derner et al., 2006). $\delta^{15}N$ values of consumers reflect a combination of trophic position and/or shifts in the baseline nitrogen isotope composition of primary producers, with higher $\delta^{15}N$ values signifying higher trophic position or increased aridity (DeNiro and Epstein, 1981; Ambrose, 1991; Amundson et al., 2003). Consumer tissue $\delta^{13}C$ and $\delta^{15}N$ values systematically differ from that of their diet due to physiologically mediated isotopic discrimination (Koch, 2007) and these differences are quantified as trophic discrimination factors (TDF). Thus, at a particular time interval, $\delta^{13}C$ and $\delta^{15}N$ values vary across animals in a community depending upon their trophic level and the relative proportion of $C_3$ versus $C_4$ vegetation in their diet, which allows for use of isotopic niche space of small mammals that do not move large distance as a proxy for dietary niche space (Newsome et al., 2007).

A subsample of ~150–250 mg of bone was collected from each fossil mandible or maxilla using a low-speed Dremel tool. To extract collagen, we demineralized samples with 0.25N HCl at 3–4°C for 24–48 hours. Samples were then lipid extracted via soaking in 2:1 chloroform/methanol for 72 hours, changing the solution every 24 hours. Each sample was then washed 5–7 times with distilled water and lyophilized. Approximately 0.9–1.0 mg of collagen was placed into 3 × 5mm tin capsules. Collagen $\delta^{13}C$ and $\delta^{15}N$ values were measured with a Costech elemental analyzer (Valencia, CA) interfaced with a Thermo Scientific Delta V Plus isotope ratio mass spectrometer (Bremen, Germany) at the University of New Mexico Center for Stable Isotopes (Albuquerque, NM). Isotope values are reported as δ values, where $\delta = 1000[(R_{sample}/R_{standard}) - 1]$ and $R_{samp}$ and $R_{std}$ are the $^{13}C:^{12}C$ or $^{15}N:^{14}N$ ratios of the sample and standard, respectively; units are in parts per thousand, or per mil (‰). Samples were calibrated using international reference standards; Vienna Pee Dee Belemnite (VPDB) for carbon, and atmospheric $N_2$ for nitrogen (Fry, 2006; Sharp, 2017). Analytical precision was assessed via repeated within-run analysis of organic reference materials calibrated to international standards and was determined as ≤0.2‰ for both $\delta^{13}C$ and $\delta^{15}N$ values. We also measured the weight percent carbon and nitrogen concentration of each collagen sample. Mean (±SD) [C]:[N] ratios for *Neotoma* (N = 378) were 2.9 ± 0.14 and we excluded any samples from subsequent analyses whose [C]:[N] ratios were >3.5 (Ambrose, 1990).

We followed our protocol for MNI as outlined above for the mass estimates to ensure that each sample chosen for isotope analysis represented a unique individual. Our final dataset for the isotopic analyses consisted of 306 individuals (Table 1). Not all specimens for which we had $\delta^{13}C$ and $\delta^{15}N$ measurements had body measurements, and vice versa. Of the 430 individuals with mass measurements and 306 with isotope measurements, 131 individuals had both.

### *Community, climate, and vegetation data*

We compared our body-size and isotope data with measures of the mammal community composition and turnover, climate (temperature and precipitation), and several measures of vegetation composition and change. Community data included α-diversity (richness) and β-diversity (Sorenson Index) extracted from Smith et al. (2016b), updated to reflect current phylogeny and cave fossil assembly information, and recalculated to fit within the time intervals used here (Table 1). Here, we used the Sorenson Index to calculate turnover between adjacent time intervals and similarity to the modern community composition. Turnover, defined as similarity to the previous time interval, can be used to evaluate changes in species composition between time bins and provides information on whether the presence/ absence of certain species may be affecting responses in *Neotoma*. Similarity to modern provides insight into whether species turnover is related to species permanently leaving the community and being replaced or leaving and re-entering the community through time. The original community data for Hall's Cave were compiled by Toomey (1993) and expanded to encompass the Edwards Plateau using the Neotoma Paleoecology Database (2015) by Smith et al. (2016b).

Climate information was sourced from the Community Climate System Model (CCSM3), which simulates climate across North America for the past 21,000 years (Lorenz et al., 2016a, b). The CCSM3 data have 0.5° spatial resolution, so we were able to obtain regional-scale climate for the Edwards Plateau. Mean annual maximum and minimum temperature and total mean annual precipitation data were extracted from the CCSM3 at 500 year intervals. We averaged values to the same temporal intervals used for our fossil morphometric and isotopic data (Table 1; **Figure 2**A–C).

We compared the *Neotoma* body-size and isotope data with a vegetation reconstruction from Hall's Cave based on phytolith and pollen data from 47 stratigraphic depths spanning the past 18,000 years (Cordova and Johnson, 2019). The ratio of $C_3$ to $C_4$ grasses derived from phytolith data serves as an index for the prevalence of $C_4$ grasses on the landscape, with declining $C_3$:$C_4$ values during the Holocene reflecting a shift from forests dominated by $C_3$

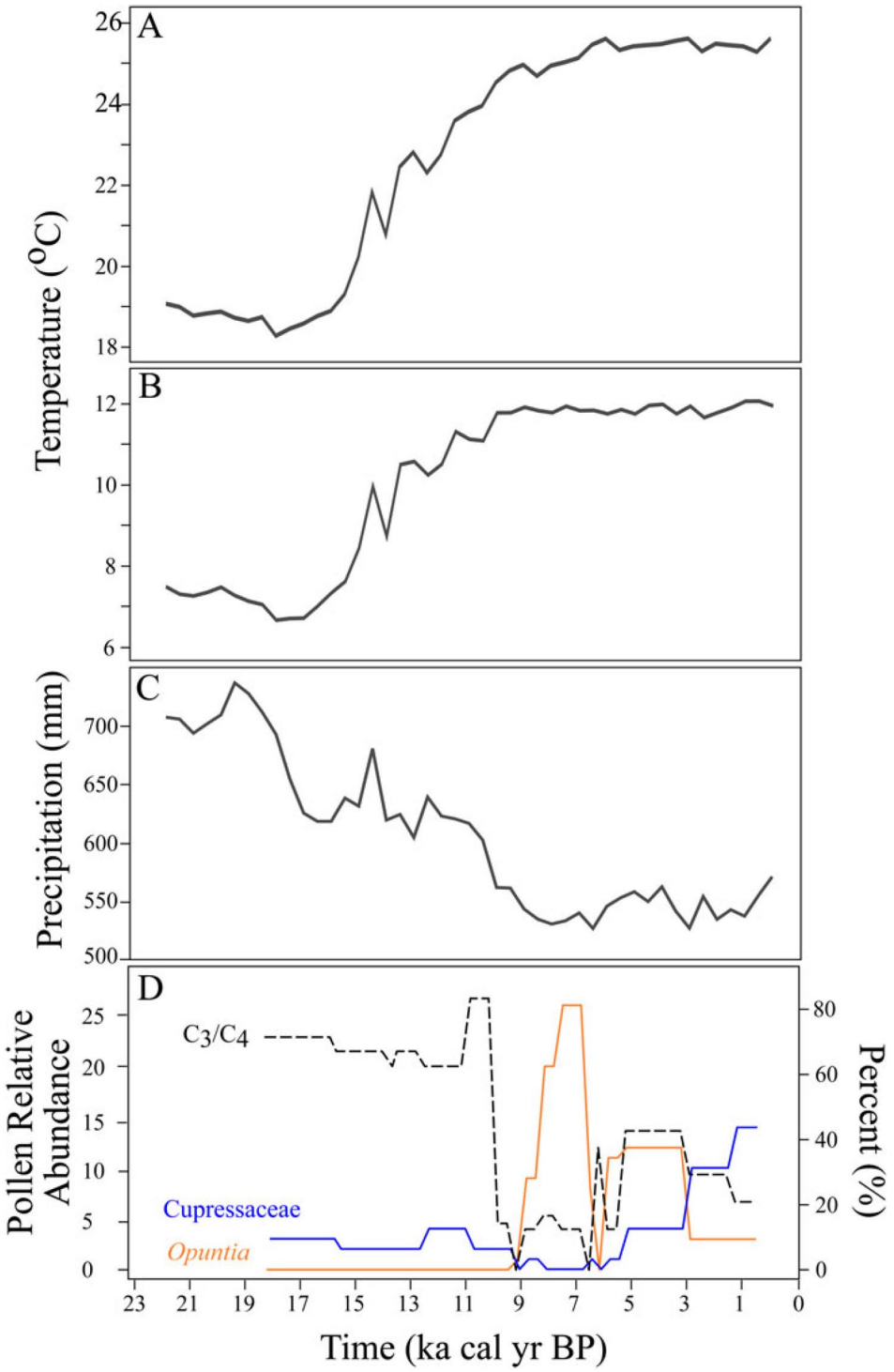


**Figure 2.**( Temporal changes in climate and vegetation on the Edwards Plateau, including (A) mean maximum temperature, (B) mean minimum temperature, and (C) mean annual precipitation (mm) (Lorenz et al., 2016a, b). (D) Pollen counts showing the relative abundance of $C_3$ versus $C_4$ (%) grasses ($C_3$ grasses/$C_4$ grasses × 100), Cupressaceae, and *Opuntia* at Hall's Cave over time (Cordova and Johnson 2019).

plants to grasslands dominated by $C_4$ grasses in response to drier conditions (Cordova and Johnson, 2019). Because modern *Neotoma albigula*, *N. floridana*, and *N. micropus* differ in their use of prickly pear cacti and juniper, we also compared our *Neotoma* data with changes in the relative abundance of *Opuntia* (prickly pear) and Cupressaceae (the family including juniper) pollen. Modern *Neotoma albigula* and *N. micropus* are known to consume prickly pear cacti, which can represent up to 45% of the annual diet of *N. albigula* (Vorhies and Taylor, 1940; Spencer and Spencer, 1941; Macêdo and Mares, 1988; Braun and Mares, 1989). Moreover, *N. albigula* makes more use of juniper than either *Neotoma floridana* or *Neotoma micropus* (Rainey, 1956; Finley, 1958; Wiley, 1980; Dial, 1988; Schmidly and Bradley, 2016). We calculated mean values of $C_3$:$C_4$ grasses in the phytolith data and mean pollen percentages for *Opuntia* and Cupressaceae for each of our 15 time intervals (Figure2D).

### *Statistical analyses*

We employed both parametric and non-parametric tests to examine changes in body mass and isotope values over time because in some instances our data violated assumptions of normality. All statistical analyses were performed using R software version R.3.6.0 (R Core Team, 2019) and RStudio 1.2.1335 (RStudio Team, 2019).

We first used an F-test and a Bartlett's test to assess changes in body mass and isotope variation before and after the extinction boundary (ca. 13,000 cal yr BP) to determine if there were marked changes associated with this period of acute biodiversity loss. To examine changes in mass across all 15 time intervals, we used ANOVA and Tukey multiple comparisons. Least squares linear regressions were also run using maximum (i.e., largest individual per time interval) and median mass against the mean $\delta^{13}C$, $\delta^{15}N$, climate, and community variables to evaluate their influence on body mass. When significant correlations were found, we conducted an analysis of covariance (ANCOVA) to assess the added effect of each on mass.

We characterized shifts in isotopic niche space using Bayesian-based standard ellipse areas ($SEA_B$) of $\delta^{13}C$ and $\delta^{15}N$, and calculated the overlap of $SEA_B$ between adjacent time intervals using the siberEllipses and maxLikOverlap functions from the SIBER package for R (Parnell and Jackson, 2013; R Core Team, 2019). We used an ANOVA to assess whether changes in $SEA_B$ were affected by sample size within time interval. The standard ellipses representing 50% of the datapoints for each time interval were plotted using JMP Pro 13 (version 13.1). Because exact trophic discrimination factors (TDFs) for *Neotoma* are not yet available, we used the SIDER package in R (Healy et al., 2018) to calculate TDFs for *Neotoma*. The SIDER package uses a dataset

of known $\Delta^{13}C$ and $\Delta^{15}N$ TDFs (Healy et al., 2017), habitat information (e.g., terrestrial), consumer diet information (e.g., herbivore), and a phylogenetic regression model to estimate the TDFs for a particular tissue type (e.g., bone collagen) of mammal or bird species (Healy et al., 2018). Using the SIDER package and dataset, we calculated the $\delta^{13}C$ diet-collagen TDFs for *Neotoma albigula* (1.9‰), *N. floridana* (1.9‰), and *N. micropus* (1.8‰), and then applied a mean (±SD) TDF of ~1.9 ± 0.5‰ for *Neotoma* at Hall's Cave. We calculated the proportion of $C_3$ in the diet of *Neotoma* for each time interval by running a mixing model in MixSIAR (Stock and Semmens, 2016) using mean $\delta^{13}C$ values for $C_3$ (−27‰) and $C_4$ (−13‰) vegetation (Boutton et al., 1998; Derner et al., 2006) and the estimated TDF. Changes in isotopic niche space were tested by analyzing $\delta_{13}C$ and $\delta^{15}N$ values using ANOVA and Tukey multiple comparisons across 14 time intervals due to lack of sufficient sample size in the oldest interval. Least squares linear regressions were run using mean, minimum, and maximum $\delta^{13}C$ and $\delta^{15}N$ against maximum and median mass, as well as climate, vegetation, and community variables.

We used a sliding window approach to test whether climate (temperature or precipitation) or community (richness or turnover) had a stronger effect on *Neotoma* at different times from the late Pleistocene to present. The sliding window consisted of six time intervals, whose start and end intervals shifted by a single interval across each iteration, for a total of 10 windows to progress across our 15 previously designated time intervals. We ran least squares linear regressions using maximum and median mass against maximum and minimum temperature, mean precipitation, species richness, turnover, and similarity to modern to determine variation in the impact of each factor between windows. For the purposes of these analyses, we assume no turnover between the community composition previous to the time interval between 22,400–15,800 cal yr BP, such that we can include all 15 time intervals and we began with a baseline of 0 for turnover.

## Results

*Neotoma* body mass did not change significantly across the extinction boundary (Supplementary Table S3; Supplementary FigureS1A), but it did decrease significantly across the 15 time intervals represented in our dataset (ANOVA F-value = 2.08, df = 14/415, $p < 0.05$: Kruskal-Wallis chi-squared = 27.24, df = 14, $p < 0.05$; Table 1; **Figure 3**A). Multiple comparisons revealed no significantly different pairs (Supplementary Table S4). Maximum body mass decreased over time, with an overall decrease from 390 g in the oldest (22,400–15,800 cal yr

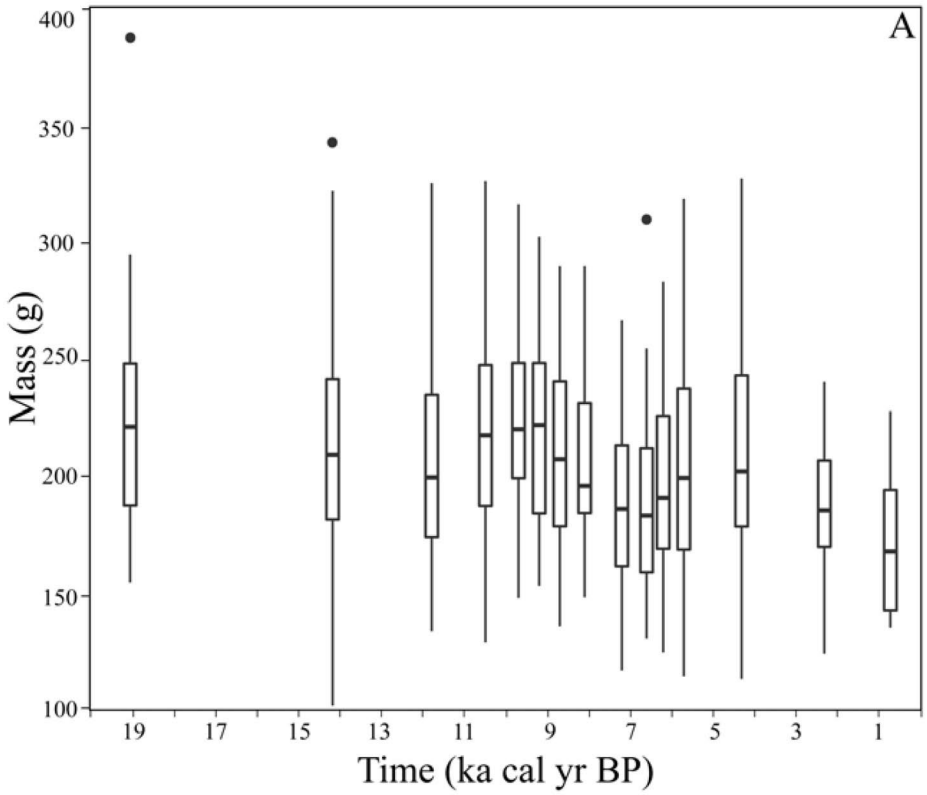
A
Mass (g)
400
350
300
250
200
150
100
19
17
15
13
11
9
7
5
3
1
Time (ka cal yr BP)

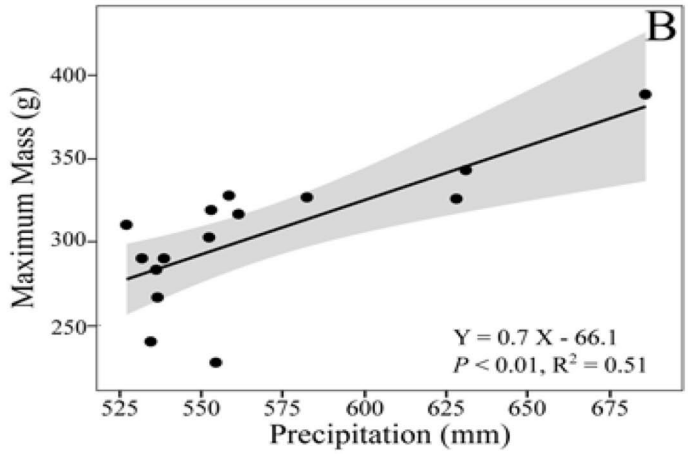
B
Maximum Mass (g)
400
350
300
250
Y = 0.7 X - 66.1
P < 0.01, R2 = 0.51
525
550
575
600
625
650
675
Precipitation (mm)

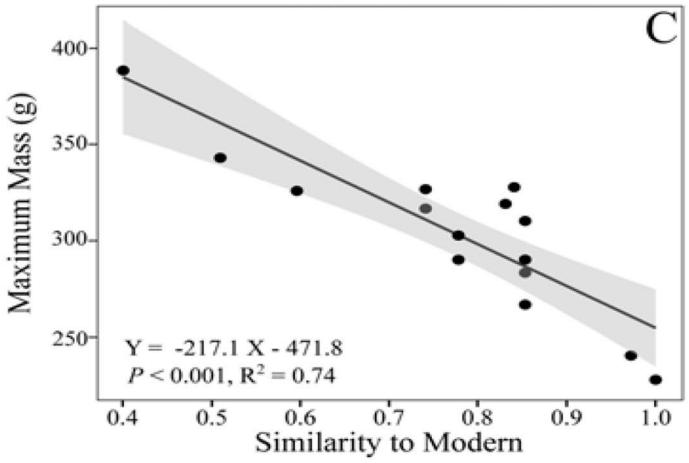
C
Maximum Mass (g)
400
350
300
250
Y = -217.1 X - 471.8
P < 0.001, R2 = 0.74
0.4
0.5
0.6
0.7
0.8
0.9
1.0
Similarity to Modern

BP) time interval to 230 g in the youngest (1500–0 cal yr BP) time interval. Changes in body mass were correlated with both climate variation and community-level shifts in species composition. Decreased maximum body mass was significantly correlated with increasing precipitation, decreased richness, turnover between time intervals, and similarity to the modern mammal community (Supplementary Table S5; Figure3B, C). Median body mass was significantly and negatively correlated to richness, turnover, and similarity to modern community composition (Supplementary Table S5). Despite the importance of both richness and turnover on body mass, increasing similarity of community composition to modern had a stronger effect on both maximum and median mass than either species turnover or richness (Supplementary Table S5). Results of ANCOVA ($F = 2.819$, $p > 0.5$), suggesting that precipitation is correlated with changes in mass independently from richness, similarity to modern, or turnover, such that maximum and median body mass decreased with community changes throughout the Holocene.

Although body mass of *Neotoma* varied significantly across time, these changes do not appear to be related to isotopic variation. Linear models found no correlation between either carbon ($\delta^{13}C$) or nitrogen ($\delta^{15}N$) values with body size (Supplementary Table S6). The sliding window analysis demonstrated that responses in maximum and median mass of *Neotoma* were generally separated across time from changes in both climate and community composition. The majority of significant correlations between maximum mass and both climate and community composition shifts were found in windows whose time intervals occurred before 6700–6400 cal yr BP. Maximum body mass prior to this interval was significantly positively related to precipitation and mammal species richness, and negatively related to maximum and minimum temperature and species turnover (Supplementary Table S7). The median mass of *Neotoma* was found to be significantly

**Figure 3.** Temporal changes in Neotoma body mass. Boxplots show the first and third quartiles, median (middle bar), with whiskers extending up to 1.5 times the interquartile range; black circles represent outliers for (A) mass of Neotoma across 15 time intervals. Linear models of maximum body size (g) versus (B) mean annual precipitation (mm) and (C) Sorenson index as similarity of community composition to the youngest time interval (modern).

and positively correlated with precipitation and negatively with turnover after 6700 cal yr BP (Supplementary Table S7). No significant relationship was found between median body mass and temperature across the 10 sliding windows.

Mean $\delta^{13}C$ and $\delta^{15}N$ values of *Neotoma* bone collagen from our 15 time intervals ranged from –16.9‰ to –19.5‰ (SD: 0.3–3.1‰) and 4.2‰ to 6.5‰ (SD: 0.9-1.7‰), respectively, with the weight percent [C]:[N] ratios of specimens between 2.7–3.5. *Neotoma* $\delta^{13}C$ and $\delta^{15}N$ values decreased across the extinction boundary ($\delta^{13}C$: ANOVA F-value = 4.96, df = 1/304, $p < 0.05$; Kruskal-Wallis chi-squared = 5.29, df = 1, p-value <0.05; $\delta^{15}N$: ANOVA F-value = 18.28, df = 1/304, p-value < 0.001; Kruskal-Wallis chi-squared =18.54, df = 1, $p < 0.001$). Variance in $\delta^{13}C$ values increased after the extinction boundary, while $\delta^{15}N$ remained similar across time (Supplementary Table S3; Supplementary FigureS1C). Mixing model results show that *Neotoma* consumed a mixed $C_3$ and $C_4$/CAM diet across the entire record, with the percent of $C_3$ resources in the diet ranging between ~40–60% (Table 1). *Neotoma* consumed the highest proportion of $C_3$ resources prior to 10,000 cal yr BP (55–60 ± 3–7%), and again at 3100–1500 cal yr BP (59 ± 8%). *Neotoma* consumed the lowest proportion (42 ± 10%) of $C_3$ resources at 7700–6700 cal yr BP (Table 1), but generally consumed 45–55 ± 8–14% $C_3$ resources after 10,000 cal yr BP. *Neotoma* consumed a significantly greater proportion of $C_4$/CAM at 7700–6700 cal yr BP than during 15,800–10,000 cal yr BP and 3100–1500 cal yr BP (ANOVA F-value = 3.14, df = 14/291, $p < 0.001$; Kruskal-Wallis chi-squared = 43.36, df = 14, $p < 0.001$; Supplementary Table S4). $\delta^{15}N$ values of *Neotoma* were significantly higher at 9000–8400 cal yr BP than during 22,400–12,700 cal yr BP (ANOVA F-value = 2.45, df = 14/291, $p < 0.01$; Kruskal-Wallis chi-squared = 34.08, df = 14, $p < 0.01$, Supplementary Table S4).

The isotopic niche space ($SEA_B$) of *Neotoma* increased over time (**Figures 4**A–C, 5; Supplementary FigureS2). We found no relationship between $SEA_B$ and sample sizes across our intervals (ANOVA F-value = 0.001, df = 1/13, $p > 0.1$). Overlap in dietary niche space was highest between ca. 3100–0, 6100–3100, and 10,000–8400 cal yr BP (Figure 4C, **Figure 5**). *Neotoma* $\delta^{13}C$ and $\delta^{15}N$ values were significantly and positively correlated, with increasing $\delta^{15}N$ values associated with a higher proportion of $C_4$/CAM resource use (Supplementary Table

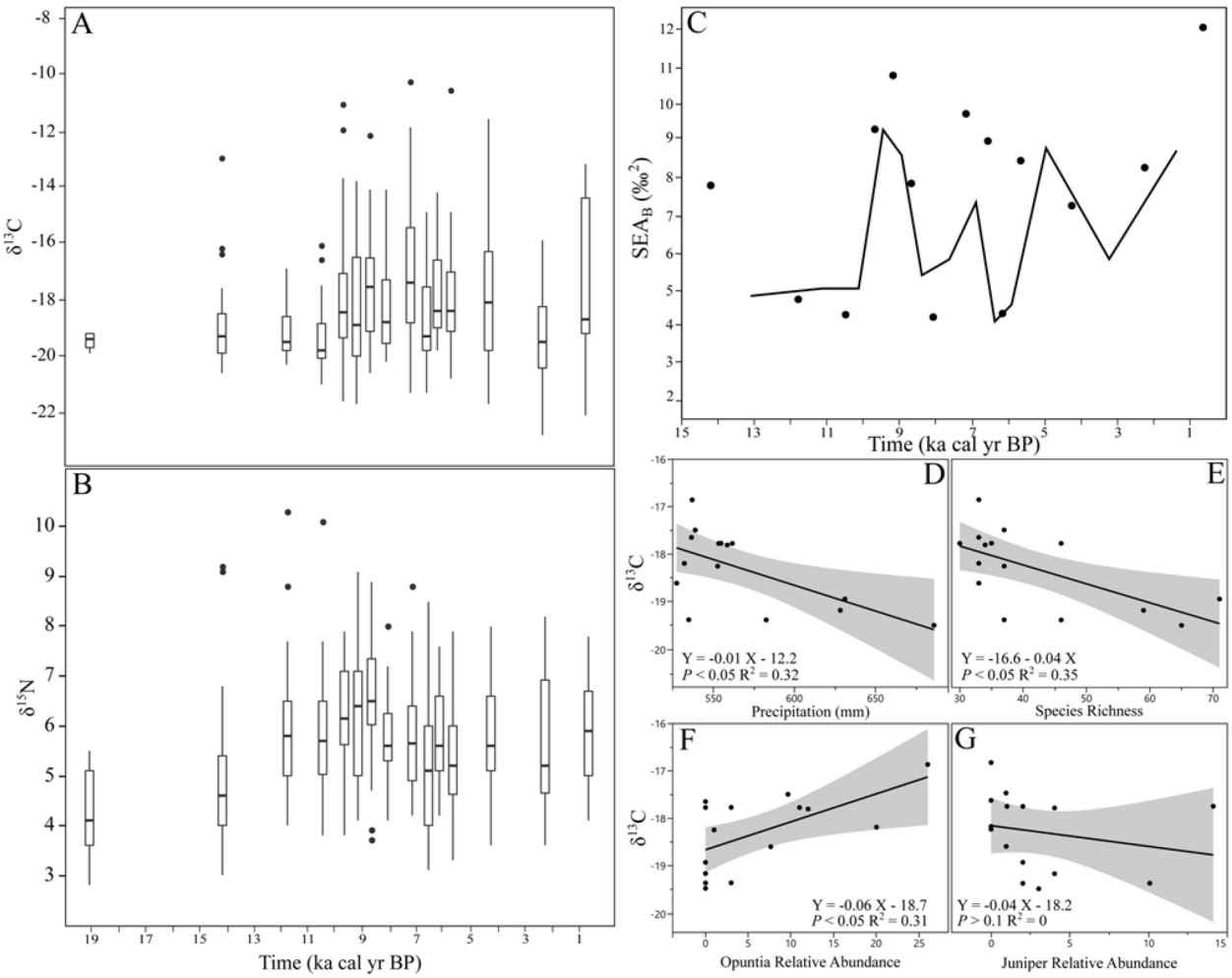


**Figure 4.** Temporal changes in Neotoma collagen isotopes. Boxplots give first and third quartiles, median, and 1.5 times the interquartile range (whiskers), with outliers (black circles) for (A) $\delta^{13}C$ and (B) $\delta^{15}N$ values. (C) Standard ellipse areas ($SEA_B$ in $‰^2$) and overlap of adjacent $SEA_B$ values (solid line) through time. Linear relationships between (D) mean annual precipitation, (E) local mammal species, relative pollen abundance of (F) *Opuntia*, and (G) Cupressaceae.

S6). Mean bone collagen $\delta^{13}C$ values were significantly and negatively correlated to precipitation and species richness (Supplementary Table S4; Figure4D, E), suggesting that *Neotoma* was consuming more $C_3$ resources under more mesic conditions and higher levels of α diversity, both of which were highest prior to the extinction event. Mean $\delta^{13}C$ values were also significantly and positively correlated with species turnover (Supplementary Table S5), indicating that *Neotoma* was

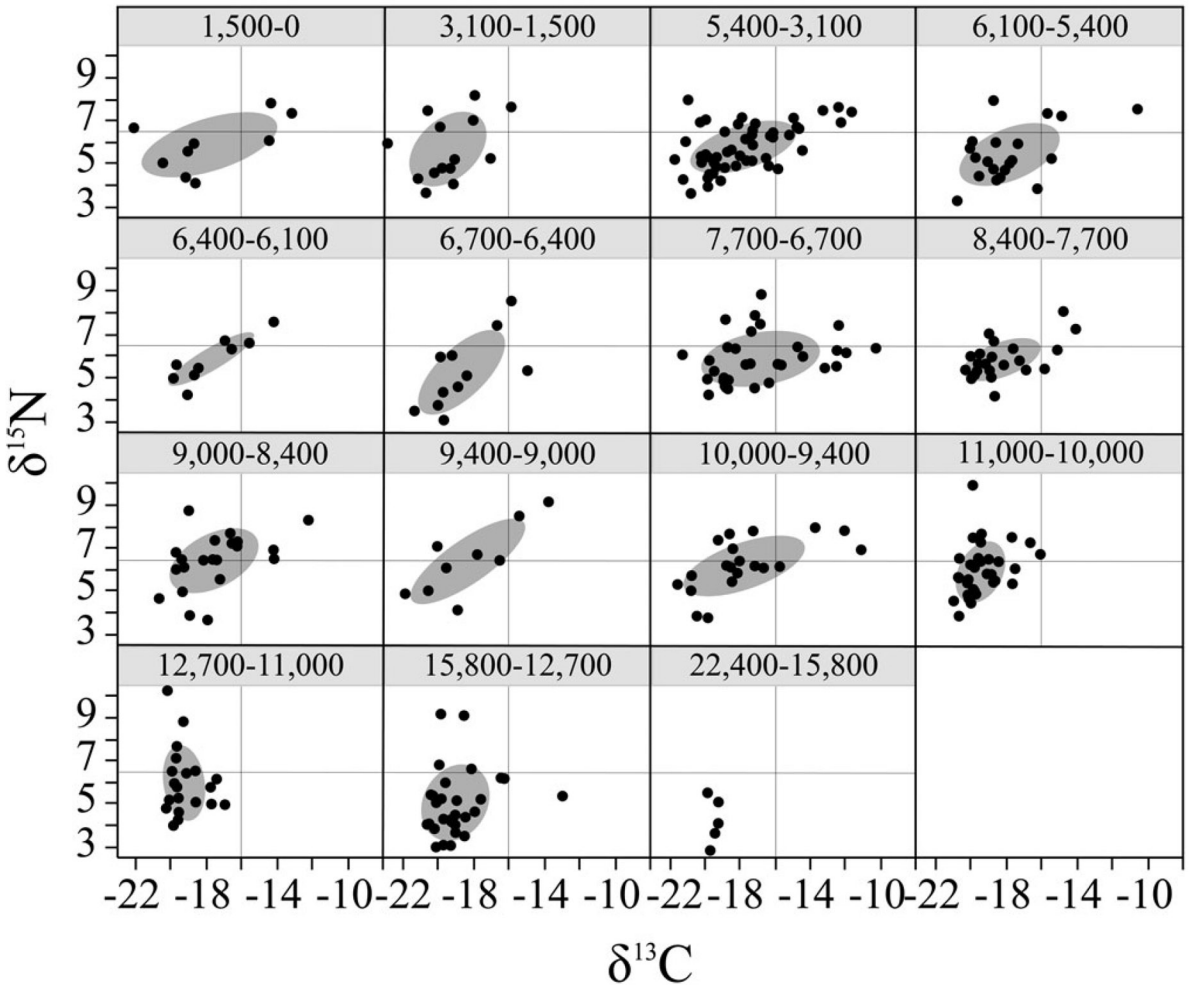


**Figure 5.** Temporal changes in the isotopic niche of *Neotoma*. Standard ellipse areas (SEAs) represent 50% coverage of population $\delta^{13}C$ and $\delta^{15}N$ values. Horizontal and vertical lines in each plot are included as a visual guide. SEA was not calculated for oldest time interval (22,400–15,800 cal yr BP) due to low sample size (N = 5).

making greater use of CAM/$C_4$ resources during periods of higher species turnover, such as during 9000–6100 cal yr BP. $\delta^{15}N$ values were significantly and negatively correlated with maximum temperature, positively correlated with minimum temperatures and precipitation, and negatively correlated with turnover (Supplementary Table S5).

$\delta^{13}C$ values were significantly correlated with changes in vegetation. *Neotoma* consumed a higher proportion of $C_4$/CAM plants, with increasing amounts of *Opuntia* (linear model F-statistic = 7.19, df = 1/13, $p < 0.05$, adjusted $r^2 = 0.31$) and decreasing amounts of $C_3$

grasses (linear model F-statistic = 9.95, df = 1/13, $p < 0.01$) on the landscape (Figure4F). We found no correlation between *Neotoma* isotope values and Cupressaceae pollen abundance (linear model F-statistic = 0.62, df = 1/13, $p > 0.1$; Figure4G).

## Discussion

Our results clearly show that *Neotoma* were sensitive to the climate and biodiversity changes of the terminal Pleistocene and early Holocene. As the glacial-era ice sheets retreated and climate warmed and dried, *Neotoma* became smaller (Figure3A) and incorporated a larger proportion of $C_4$/CAM plants in their diet as these resources increased in availability on the landscape (Figures2D, 4F, 5). Decreased body size and greater mixed resource use also were associated with the loss and turnover in mammalian biodiversity (Supplementary Table S5; Figures3C, 4E). Whether these changes resulted from adaptation within a single species, as has been shown elsewhere (Brown and Lee, 1969; Smith et al., 1995, 1998; Smith and Betancourt, 1998, 2003), or from the partial or full replacement of species within the genus is unclear, but overall we observed large shifts in the ecology of *Neotoma* as they responded to a combination of abiotic and biotic stressors.

*Neotoma* underwent significant decreases in body mass throughout the end of the Pleistocene and the Holocene (Figure3A). The decrease in the maximum body mass of *Neotoma* over time was predominantly associated with community composition becoming more similar to modern and decreasing regional precipitation (Figure3B, C; Supplementary Table S5). While greater precipitation was associated with large median and maximum body mass throughout most of the Hall's Cave record, increasing temperatures had a strong influence on decreasing maximum body mass during the time intervals prior to ca. 7000 cal yr BP, when individuals of the largest species (*N. floridana*) were likely most abundant. With the warming climate of the Holocene, thermal intolerance likely led to reduced body size in the largest individuals of *Neotoma* across time intervals, consistent with Bergmann's rule, as has been observed previously at other localities (Brown and Lee, 1969; Smith et al., 1995, 1998; Smith and Betancourt, 1998, 2003). The influence of community turnover on both maximum

and median body mass suggests that animals became smaller overall as the mammal community composition became more similar to modern (Supplementary Table S5). Decreased size may be advantageous for predator avoidance in small mammals (Stanley, 1973), or smaller size may have altered *Neotoma*'s ability to compete for resources or habitat, given that larger size in modern *Neotoma* can act as a competitive advantage (Finley, 1958; Cameron, 1971; Dial, 1988). Smaller body mass in *Neotoma* may therefore have led to changes in biotic interactions, specifically intra- or interspecific resource competition, and contributed to observed shifts in diet.

The dietary (isotopic) niche of *Neotoma* also shifted across the past 22,000 years with changes in climate, biodiversity loss, and vegetation. The mean $\delta^{13}C$ values of *Neotoma* across the entire temporal record at Hall's Cave were generally reflective of mixed use of $C_3$ and $C_4$/CAM resources ranging between –16.9 to –19.5‰ (SD: 0.3–3.1‰) (Table 1). The largest $\delta^{13}C$ change occurs around the extinction event when *Neotoma* shift between consuming a greater proportion of $C_3$ plants prior to the extinction to higher mixed $C_3$-$C_4$/CAM use during the Holocene (Table 1). Prior to 14,000 cal yr BP, the Edwards Plateau was covered in deciduous forest (Bryant and Holloway, 1985), but a regional shift to warmer and drier conditions led to the expansion of grassland and oak savanna ecosystems by ca. 11,600 cal yr BP (Bryant and Holloway, 1985). Over the Holocene, the Edwards Plateau became a more open savanna landscape and $C_4$ vegetation continued to increase across Texas (Nordt et al., 1994; Koch et al., 2004; Cotton et al., 2016; Cordova and Johnson, 2019). These changes occurred in concert with an increase in the isotopic niche ($SEA_B$) of *Neotoma* beginning 10,000 years ago. Prior to this interval, $C_3$ resources were ~55–60% of the diet of *Neotoma*, but use of $C_3$ plants decreased slightly (to ~42–54%) for most of the Holocene, with the exception of 3100–1500 cal yr BP, when diet consisted of 59% $C_3$ resources (Table 1). Following an increase in *Opuntia* abundance at ca. 9000 cal yr BP (Cordova and Johnson, 2019; Figure2D), we find a parallel increase in the consumption of $C_4$/CAM (58%) at 7700–6700 cal yr BP. A sudden decrease in $SEA_B$ between 6700–6400 cal yr BP (Figure4C; 5) coincides with the disappearance of *Opuntia* from the Hall's Cave fossil record (Fig 2D), and a shift away from a more mixed $C_3$-$C_4$/CAM diet to greater use of $C_3$ resources (~54%, Table 1). As *Opuntia* reappears,

the breadth of $\delta^{13}C$ values of *Neotoma* increase as well (Figures2D, 4C, 5). These patterns suggest a strong influence of local vegetation composition and resource availability on the diet of *Neotoma*.

Temporal variation in *Neotoma* $\delta^{15}N$ values (Figures4B, 5) potentially reflect changes in trophic level and/or baseline shifts in the nitrogen isotope composition of vegetation. Here, $\delta^{15}N$ values of *Neotoma* collagen decreased over time and were positively correlated with higher $\delta^{13}C$ values (Figures4B, 5). Tomé et al. (2020a) found a similar pattern in the $\delta^{15}N$ values for *Sigmodon hispidus* (hispid cotton rat) in the Hall's Cave record, an herbivorous rodent generally inhabiting grassland habitats (Cameron and Spencer, 1981; Kincaid and Cameron, 1985; Randolph et al., 1991; Toomey, 1993). *Sigmodon* $\delta^{15}N$ values ranged between 5.5–7.4‰, and throughout the 14 time intervals that *Sigmodon* and *Neotoma* co-occur, their mean $\delta^{15}N$ values were within 2‰ of each other and they had a similar degree of within-interval variance, suggesting they were likely feeding at similar trophic levels. *Sigmodon* was strongly influenced by shifts in community composition and resource availability such that the decrease in $\delta^{15}N$ values in this omnivorous generalist corresponded with an increase in the proportion of insectivores on the landscape (Tomé et al., 2020a). Interestingly, a significant correlation between *Neotoma* $\delta^{15}N$ and turnover (negative correlation) and similarity to modern (positive correlation) species composition in the community suggest that changes in resource use by *Neotoma* were linked to biotic interactions (i.e., competition). Omnivory in modern populations of *Neotoma*, however, is restricted to a very limited consumption of insects (Vorhies and Taylor, 1940; Rainey, 1956). The $\delta^{15}N$ values of a consumer are typically enriched by ~3–5‰ compared to its diet (DeNiro and Epstein, 1981), and on the whole, the mean $\delta^{15}N$ values of *Neotoma* varied by only 2.3‰ across all intervals, with the SD for any given time interval being below 2‰, suggesting the genus was unlikely to be switching between omnivorous and herbivorous diets. Comparison of *Neotoma* $\delta^{15}N$ data with those of other obligate herbivores suggests that this degree of variation in $\delta^{15}N$ is common in primary consumers. For example, bison $\delta^{15}N$ values were 5.7–8.3‰ (±0.7–1.2‰) between ca. 6000– 3100 cal yr BP and 5.7–6.2‰ (±0.5–0.9‰) between ca. 3100– 500 cal yr BP across seven Texas cave sites (Lohse et al., 2014), while *Neotoma* $\delta^{15}N$ values were 5.4–5.8‰ (±1.1–1.3‰) between ca.

6100–3100 cal yr BP and 5.7–5.9‰ (±1.3–1.5‰) between ca. 3100–0 cal yr BP. *Bison* also show a positive correlation between $\delta^{13}C$ and $\delta^{15}N$ values and a significant decrease in $\delta^{15}N$ values over the Holocene (Lohse et al., 2014). The small range in *Neotoma* $\delta^{15}N$ values and the correlation between increased $C_4$ consumption and higher $\delta^{15}N$ values in many time bins (Figures4B, 5) could therefore result from changing environmental conditions (DeNiro and Epstein, 1981; Amundson et al., 2003). In general, plant $\delta^{15}N$ values increase with environmental aridity (Ambrose, 1991; Austin and Vitousek, 1998; Amundson et al., 2003). We found *Neotoma* $\delta^{15}N$ values were positively correlated with increasing minimum temperature, suggesting plant $\delta^{15}N$ increased as the environment warmed. However, we also found $\delta^{15}N$ decreased with increasing maximum temperature, and we found no correlation between $\delta^{15}N$ and precipitation (Supplementary Table S5), as may have been expected from modern patterns. Despite this, the lack of evidence for a trophic level shift and the similar patterns shown in herbivore nitrogen values from the region suggest changes in $\delta^{15}N$ values of *Neotoma* at Hall's Cave were likely due to changes in the baseline nitrogen isotope composition of local vegetation.

Shifts in both body mass and diet of *Neotoma* also may be related to temporal changes in the species of *Neotoma* that were present at the site. Prior to the extinction event, the larger-bodied *N. floridana* was most likely the only species present, according to DNA work on fossils from the oldest strata (Seersholm et al., 2020). From ca. 21,000–17,000 cal yr BP, the vegetation of the Edwards Plateau was deciduous forest, which is the preferred habitat for modern *N. floridana* (Rainey, 1956; Bryant and Holloway, 1985). After 17,000 cal yr BP, the region shifted towards a more open grassland/savanna habitat (Bryant and Holloway, 1985; Cordova and Johnson, 2019), which is more characteristic of the habitat within the modern range of *N. micropus* and/or *N. albigula* (Finley, 1958; Macêdo and Mares, 1988; Braun and Mares, 1989). Rapid decreases in precipitation and increasing temperature before ca. 9000 cal yr BP (Figure2A–C) were strongly correlated with decreases in maximum body mass (Supplementary Table S5) and may be a result of a lower abundance of *N. floridana* on the landscape. Increasing similarity of mammal species to modern community composition was also significantly and positively correlated to maximum body mass prior to ca. 7000 cal yr BP and to median body mass after

ca. 9000–7000 cal yr BP, suggesting an important transition in the abundance and composition of *Neotoma* species present on the Edwards Plateau. Thus, colonization of the Edwards Plateau by smaller *Neotoma* species may have been facilitated by regional shifts in vegetation due to changing climate. The observed decrease in *Neotoma* body mass may be a consequence of an adaptation to increasing temperatures, but may also be related to the increased abundance of *N. micropus* and/or *N. albigula* in the Hall's Cave fossil record.

Changes in diet of *Neotoma* over time also may be related to differences in resource use among species in the genus. Today, both *N. albigula* and *N. micropus* consume high proportions of cacti (e.g., *Opuntia*; Finley, 1958; Dial, 1988; Macêdo and Mares, 1988; Braun and Mares, 1989). Drought-adapted CAM plants typically have $\delta^{13}C$ values that are similar to $C_4$ plants in arid land ecosystems; mean (±SE) $\delta^{13}C$ values for *Opuntia* (prickly pear cacti) collected in Texas south of the Edwards Plateau were –15.6 ± 0.2‰ (Mooney et al., 1974; Sutton et al., 1976; Mooney et al., 1989; Boutton et al., 1998). We found a significant and positive correlation between the increase in the amount of the *Opuntia* cactus in the region with (1) decreased precipitation (Figure2), and (2) higher *Neotoma* $\delta^{13}C$ values (Figure4F). This shift in the $\delta^{13}C$ values of *Neotoma* is indicative of greater use of $C_4$/CAM resources. Additionally, regional vegetation shifts may have decreased the habitat and resources that *N. floridana* relies on for den building (e.g., fallen tree trunks and branches), and increased those (e.g., shrubs and cacti) used by *N. micropus* and/or *N. albigula* (Rainey, 1956; Finley, 1958; Brown et al., 1972; Thies and Caire, 1990). Reduced availability of appropriate building materials for den construction can lead to declines in modern *Neotoma* populations, generally related to reduced thermal and predator protection (Raun, 1966; Brown, 1968; Brown et al., 1972; Smith, 1995b; Ford et al., 2006). We also found that while the presence of cacti was significantly correlated with shifts in *Neotoma* diet, juniper (Cupressaceae) abundance was not. Of these three species, *N. albigula* makes the most use of juniper, which can represent as much as 35% of the diet in some populations (Finley, 1958). The lack of correlation with changes in juniper and diet (Figure4G) may suggest that *N. albigula* was present in lower abundance than *N. micropus* in the Hall's Cave record after ca. 6700 cal yr BP, potentially because the larger-bodied *N. micropus* outcompeted

smaller-bodied species for space and resources (Finley, 1958; Cameron, 1971; Dial 1988). We also found no overall correlation between body size and diet (Supplementary Table S6), despite shifts towards smaller size and higher $C_4$/CAM consumption over time. It is possible that variation in resource use within one or more species of *Neotoma* is partially responsible for change in $\delta^{13}C$ values, as shown by small-mammal studies that reported wide resource use even in what are considered to be dietary specialists (Terry et al., 2017, Terry, 2018). However, if *N. micropus* abundances were higher than those *N. albigula*, the larger overlap in mass with co-occurring *N. floridana* may mask changes at the species level versus wider resource use at the genus level.

Overall, *Neotoma* responses suggest a strong abiotic influence from climate at the terminal Pleistocene, and likely changes in relative abundance from *N. floridana* to *N. micropus* and/or *N. albigula* in the Holocene associated with changing local resource availability. Climatic fluctuations and ecosystem disruption due to the megafauna extinction event may both have played roles in vegetation shifts (Owen-Smith, 1992), which led to a change in relative abundances of *Neotoma* species as habitat and resources became more suitable to the two arid-adapted species. Differences in how *Neotoma* responded to community and climatic changes across the Hall's Cave record suggest that the strength of abiotic and biotic effects on a species can vary over time. Characterization of a genus' or species' niche(s) through time can therefore provide insight into the regional vegetational and community shifts produced as a consequence of large-scale abiotic and biotic changes, which can inform how modern communities may respond to modern anthropogenic climate change and biodiversity loss.

**Supplementary Material.** The supplementary material for this article can be found following the References or attached to the archive record.

**Acknowledgments** We thank the staff at the Texas Memorial Museum for access to their fabulous collections and their expertise and help; we are particularly grateful to Drs. Chris Sagebiel and Ernie Lundelius for their willingness to assist us with locating references, specimens, and information about the sites. We also thank Dr. Thomas W. Stafford Jr. at Stafford Research for his input, enthusiasm, and work with the Hall's Cave fossil record; this project would not have been possible without his assistance. The Museum of Southwestern Biology and the Senior Collection Manager of Mammals, Dr. Jon Dunnum, provided access to the modern collections at UNM. We would also like to thank Dr. Rickard Toomey for his foundational excavations and work at Hall's Cave, which made our project possible, and the owners of the private ranch on which Hall's Cave is located for having graciously allowed generations of paleontologists to work at this very important late Quaternary fossil site. Finally, thanks to the many members of the Smith lab at UNM, especially Jonathan Keller, who assisted with revisions of the age model. Financial Support. Funding for this project was provided by NSF-DEB 1555525 and 1744223 (FA Smith, PI; SD Newsome, SK Lyons co-PIs). Data Availability. Data are available from the Dryad Digital Repository: Tomé, Catalina P.; Lyons, S. Kathleen; Newsome, Seth D.; Smith, Felisa A. (2021), Data from: The sensitivity of *Neotoma* to climate change and biodiversity loss over the late Quaternary, Dryad, Dataset, https://doi.org/105061/dryad.4jozpc8b3 .

## References

Alley, R.B., 2000. The Younger Dryas cold interval as viewed from central Greenland. *Quaternary Science Reviews* 19, 213–226.

Ambrose, S.H., 1990. Preparation and characterization of bone and tooth collagen for isotopic analysis. *Journal of Archaeological Science* 17, 431–451.

Ambrose, S.H., 1991. Effects of diet, climate and physiology on nitrogen isotope abundances in terrestrial foodwebs. *Journal of Archaeological Science* 18, 293–317.

Amundson, R., Austin, A.T., Schuur, E.A., Yoo, K., Matzek, V., Kendall, C., Uebersax, A., Brenner, D., Baisden, W.T., 2003. Global patterns of the isotopic composition of soil and plant nitrogen. *Global Biogeochemical Cycles* 17, 1031. https://doi.org/10.1029/2002GB001903

Andrewartha, H.G., Birch, L.C., 1986. *The Ecological Web: More on the Distribution and Abundance of Animals*. University of Chicago Press, Chicago.

Ashton, K.G., Tracy, M.C., Queiroz, A.D., 2000. Is Bergmann's rule valid for mammals? *American Naturalist* 156, 390–415.

Auffray, J.C., Renaud S., Claude, J., 2009. Rodent biodiversity in changing environments. *Kasetsart Journal, Natural Science* 43, 83–93.

Austin, A.T., Vitousek, P.M., 1998. Nutrient dynamics on a precipitation gradient in Hawai'i. *Oecologia* 113, 519–529.

Bakker, E.S., Gill, J.L., Johnson, C.N., Vera, F.W., Sandom, C.J., Asner, G.P., Svenning, J.C., 2016. Combining paleo-data and modern exclosure experiments to assess the impact of megafauna extinctions on woody vegetation. *Proceedings of the National Academy of Sciences* 113, 847–855.

Barnosky, A.D., Lindsey, E.L., Villavicencio, N.A., Bostelmann, E., Hadly, E.A., Wanket, J., Marshall, C.R., 2016. Variable impact of late-Quaternary megafaunal extinction in causing ecological state shifts in North and South America. *Proceedings of the National Academy of Sciences* 113, 856–861.

Bergmann, C., 1847. Über die Verhältnisse der Wärmeökonomie der Thiere zu ihrer Größe. *Göttinger Studien* 3, 595–708.

Blois, J.L., McGuire, J.L., Hadly, E.A., 2010. Small mammal diversity loss in response to late-Pleistocene climatic change. *Nature* 465, 771–774.

Bourne, M.D., Feinberg, J.M., Stafford Jr, T.W., Waters, M.R., Lundelius Jr, E., Forman, S.L., 2016. High-intensity geomagnetic field 'spike' observed at ca. 3000 cal BP in Texas, USA. *Earth and Planetary Science Letters* 442, 80-92.

Boutton, T.W., Archer, S.R., Midwood, A.J., Zitzer, S.F., Bol, R., 1998. δ13C values of soil organic carbon and their use in documenting vegetation change in a subtropical savanna ecosystem. *Geoderma* 82, 5–41.

Boutton, T.W., Nordt, L.C., Archer, S.R., Midwood, A.J., Casar, I., 1993. Stable carbon isotope ratios of soil organic matter and their potential use as indicators of palaeoclimate. In: *Proceedings of the International Symposium on Applications of Isotope Techniques in Studying Past and Current Environmental Changes in the Hydrosphere and the Atmosphere*. International Atomic Energy Agency, no. 329, pp. 445–459.

Bowers, M.A., Brown, J.H., 1982. Body size and coexistence in desert rodents: chance or community structure? *Ecology* 63, 391–400.

Braun, J.K., Mares, M.A., 1989. *Neotoma micropus*. *Mammalian Species* 330, 1–9.

Brown, J.H., 1968. Adaptation to environmental temperature in two species of woodrats, *Neotoma cinerea* and *N. albigula*. *Miscellaneous Publications, Museum of Zoology, University of Michigan* 135, 1–48.

Brown, J.H., 1973. Species diversity of seed-eating desert rodents in sand dune habitats. *Ecology* 54, 775-787.

Brown, J.H., Heske, E.J., 1990. Temporal changes in a Chihuahuan Desert rodent community. *Oikos* 59, 290–302.

Brown, J.H., Lee, A.K., 1969. Bergmann's rule and climatic adaptation in woodrats (*Neotoma*). *Evolution* 23, 329–338.

Brown, J.H., Lieberman, G.A., Dengler, W.F., 1972. Woodrats and cholla: dependence of a small mammal population on the density of cacti. *Ecology* 53, 310–313.

Brown, J.H., Nicoletto, P.F., 1991. Spatial scaling of species composition: body masses of North American land mammals. *The American Naturalist* 138, 1478–1512.

Bryant, V.M., Jr., Holloway, R.G., 1985. A late-Quaternary paleoenvironmental record of Texas: an overview of the pollen evidence. In: Bryant, V.M., Jr., Holloway, R.G. (Eds.), *Pollen Records of Late-Quaternary North American Sediments*. American Association of Stratigraphic Palynologists Foundation, Dallas, TX, pp. 39–70.

Cameron, G.N., 1971. Niche overlap and competition in woodrats. *Journal of Mammalogy* 52, 288–296.

Cameron, G.N., Spencer, S.R., 1981. *Sigmodon hispidus*. *Mammalian Species* 158, 1–9.

Carraway, L.N., Verts, B.J., 1991. *Neotoma fuscipes*. *Mammalian Species* 386, 1–10.

Cerling, T. E., Harris, J.M., MacFadden, B.J., Leakey, M.G., Quade, J., Eisenmann, V., Ehleringer, J.R., 1997. Global vegetation change through the Miocene/Pliocene boundary. *Nature* 389, 153–158.

Chamberlain, C.P., Waldbauer, J.R., Fox-Dobbs, K., Newsome, S.D., Koch, P.L., Smith, D.R., Church, M.E., et al., 2005. Pleistocene to recent dietary shifts in California condors. *Proceedings of the National Academy of Sciences* 102, 16707–16711.

Cole, K.L., Arundel, S.T., 2005. Carbon isotopes from fossil packrat pellets and elevational movements of Utah agave plants reveal the Younger Dryas cold period in Grand Canyon, Arizona. *Geology* 33, 713–716.

Cooke, M.J., Stern, L.A., Banner, J.L., Mack, L.E., Stafford Jr, T.W., Toomey III, R.S., 2003. Precise timing and rate of massive late Quaternary soil denudation. *Geology* 31, 853–856.

Cordova, C.E., Johnson, W.C. 2019. An 18 ka to present pollen- and phytolith-based vegetation reconstruction from Hall's Cave, south-central Texas, USA. *Quaternary Research* 92, 497–518.

Cotton, J.M., Cerling, T.E., Hoppe, K.A., Mosier, T.M., Still, C.J., 2016. Climate, CO2, and the history of North American grasses since the Last Glacial Maximum. *Science Advances* 2, e1501346. https://doi.org/10.1126/sciadv.1501346

Damuth, J., 1981. Population density and body size in mammals. *Nature* 290, 699–700.

Dansgaard, W., White, J.W.C., Johnsen, S.J., 1989. The abrupt termination of the Younger Dryas climate event. *Nature* 339, 532–534.

Dearing, M.D., McLister, J.D., Sorensen, J.S., 2005. Woodrat (*Neotoma*) herbivores maintain nitrogen balance on a low-nitrogen, high-phenolic forage, *Juniperus monosperma*. *Journal of Comparative Physiology B* 175, 349–355.

DeNiro, M.J., Epstein, S., 1978. Influence of diet on the distribution of carbon isotopes in animals. *Geochimica et Cosmochimica Acta* 42, 495–506.

DeNiro, M.J., Epstein, S., 1981. Influence of diet on the distribution of nitrogen isotopes in animals. *Geochimica et Cosmochimica Acta* 45, 341–351.

Derner, J.D., Boutton, T.W., Briske, D.D., 2006. Grazing and ecosystem carbon storage in the North American Great Plains. *Plant and Soil* 280, 77–90.

Dial, K.P., 1988. Three sympatric species of *Neotoma*: dietary specialization and coexistence. *Oecologia* 76, 531–537.

Doughty, C.E., Wolf, A., Malhi, Y., 2013. The legacy of the Pleistocene megafauna extinctions on nutrient availability in Amazonia. *Nature Geoscience* 6, 761–764.

Dublin, H.T., Sinclair, A.R., McGlade, J., 1990. Elephants and fire as causes of multiple stable states in the Serengeti-Mara woodlands. *The Journal of Animal Ecology* 59, 1147–1164.

Farquhar, G.D., Ehleringer, J.R., Hubick, K.T., 1989. Carbon isotope discrimination and photosynthesis. *Annual Review of Plant Biology* 40, 503–537.

Finley, R.B., 1958. The wood rats of Colorado, distribution and ecology. *University of Kansas Publications of the Museum of Natural History* 10, 213–552.

Ford, W.M., Castleberry, S.B., Mengak, M.T., Rodrigue, J.L., Feller, D.J., Russell, K.R., 2006. Persistence of Allegheny woodrats *Neotoma magister* across the mid-Atlantic Appalachian Highlands landscape, USA. *Ecography* 29, 745–754.

Freckleton, R.P., Harvey, P.H., Pagel, M., 2003. Bergmann's rule and body size in mammals. *The American Naturalist* 16, 821–825. Fry, B., 2006. *Stable Isotope Ecology*. Springer, New York.

Galetti, M., Guevara, R., Neves, C.L., Rodarte, R.R., Bovendorp, R.S., Moreira, M., Hopkins, J.B., III, Yeakel, J.D., 2015. Defaunation affect population and diet of rodents in Neotropical rainforests. *Biological Conservation* 190, 2–7.

Goheen, J.R., Augustine, D.J., Veblen, K.E., Kimuyu, D.M., Palmer, T.M., Porensky, L.M., Pringle, R.M., et al., 2018. Conservation lessons from large-mammal manipulations in East African savannas: the KLEE, UHURU, and GLADE experiments. *Annals of the New York Academy of Sciences* 1429, 31–49.

Goheen, J.R., Keesing, F., Allan, B.F., Ogada, D., Ostfeld, R.S., 2004. Net effects of large mammals on *Acacia* seedling survival in an African savanna. *Ecology* 85, 1555–1561.

Goheen, J.R., Palmer, T.M., Keesing, F., Riginos, C., Young, T.P., 2010. Large herbivores facilitate savanna tree establishment via diverse and indirect pathways. *Journal of Animal Ecology* 79, 372–382.

Graham, R.W., 1987. Late Quaternary mammalian faunas and paleoenvironments of the southwestern Plains of the United States. In: Graham, R.W., Semken, H.A., Jr., Graham, M.A. (Eds.), *Late Quaternary mammalian biogeography and environments of the Great Plains and Prairies*. Illinois State Museum Scientific Papers 22, pp. 24–86.

Graham, R.W., Lundelius, E.L., Jr., Graham, M.A., Schroeder, E.K., Toomey, R.S., III, Anderson, E., Barnosky, A.D., et al., 1996. Spatial response of mammals to late Quaternary environmental fluctuations. *Science* 5208, 1601–1606.

Grayson, D.K., 2000. Mammalian responses to middle Holocene climatic change in the Great Basin of the western United States. *Journal of Biogeography* 27, 181–192.

Healy, K., Guillerme, T., Kelly, S.B., Inger, R., Bearhop, S., Jackson, A.L., 2017. Data from: SIDER: an R package for predicting trophic discrimination factors of consumers based on their ecology and phylogenetic relatedness. *Dryad Digital Repository*. http://dx.doi.org/10.5061/dryad.c6035

Healy, K., Guillerme, T., Kelly, S.B., Inger, R., Bearhop, S., Jackson, A.L., 2018. SIDER: an R package for predicting trophic discrimination factors of consumers based on their ecology and phylogenetic relatedness. *Ecography* 41, 1393–1400.

IPCC, 2014. *Climate Change 2014: Synthesis Report. Contribution of Working Groups I, II and III to the Fifth Assessment Report of the Intergovernmental Panel on Climate Change* (Core Writing Team, Pachauri, R.K., Meyer, L.A. [Eds.]). Intergovernmental Panel on Climate Change (IPCC), Geneva, Switzerland, 151 pp.

Janzen, D H., Martin, P.S., 1982. Neotropical anachronism: the fruits the Gomphotheres ate. *Science* 215, 19–27.

Johnson, C.N., 2009. Ecological consequences of Late Quaternary extinctions of megafauna. *Proceedings of the Royal Society B: Biological Sciences* 276, 2509–2519.

Joines, J.P., 2011. *17,000 Years of Climate Change: the Phytolith Record from Hall's Cave, Texas*. MS thesis, Oklahoma State University, Stillwater, Oklahoma, USA, 35 pp.

Justice, K.E., Smith, F.A., 1992. A model of dietary fiber utilization by small mammalian herbivores with empirical results for *Neotoma*. *The American Naturalist* 139, 398–416.

Keesing, F., 1998. Impacts of ungulates on the demography and diversity of small mammals in central Kenya. *Oecologia* 116, 381–389.

Keesing, F., Young, T.P., 2014. Cascading consequences of the loss of large mammals in an African savanna. *Bioscience* 64, 487–495.

Kincaid, W.B., Cameron, G.N., 1985. Interactions of cotton rats with a patchy environment: dietary responses and habitat selection. *Ecology* 66, 1769– 1783.

Koch, P.L., 2007. Isotopic study of the biology of modern and fossil vertebrates. In: Michener, R., Lajtha, K. (Eds.), *Stable Isotopes in Ecology and Environmental Science 2nd Ed*. Blackwell Publishing, Malden, MA, pp. 99–154.

Koch, P.L., Diffenbaugh, N.S., Hoppe, K.A., 2004. The effects of late Quaternary climate and $pCO_2$ change on $C_4$ plant abundance in the southcentral United States. *Palaeogeography, Palaeoclimatology, Palaeoecology* 207, 331–357.

Koch, P.L., Fox-Dobbs, K.E.N.A., Newsome, S.D., 2009. The isotopic ecology of fossil vertebrates and conservation paleobiology. In: Dietl, G.P., Flessa, K.W., *Conservation Paleobiology: Using the Past to Manage for the Future*. The Paleontological Society Papers 15, 96–112.

Koerner, S.E., Burkepile, D.E., Flynn, R.W.S., Burns, C.E., Eby, S., Govender, N., Hagenah, N., et al., 2014. Plant community response to loss of large herbivores differs between North American and South African savanna grasslands. *Ecology* 95, 808–816.

Leonard, J.A., Vilà, C., Fox-Dobbs, K., Koch, P.L., Wayne, R.K., Van Valkenburgh, B., 2007. Megafaunal extinctions and the disappearance of a specialized wolf ecomorph. *Current Biology* 17, 1146–1150.

Lohse, J.C., Madsen, D.B., Culleton, B.J., Kennett, D.J., 2014. Isotope paleoecology of episodic mid-to-late Holocene bison population expansions in the Southern Plains, U.S.A. *Quaternary Science Reviews* 102, 14–26.

Lorenz, D.J., Nieto-Lugilde, D., Blois, J.L., Fitzpatrick, M.C., Williams, J.W., 2016a. Downscaled and debiased climate simulations for North America from 21,000 years ago to 2100 AD. *Scientific Data* 3, 160048. https://doi.org/10.1038/sdata.2016.48

Lorenz, D.J., Nieto-Lugilde, D., Blois, J.L., Fitzpatrick, M.C., Williams, J.W., 2016b. Data from: downscaled and debiased climate simulations for North America from 21,000 years ago to 2100 AD. *Dryad Digital Repository*. http://dx.doi.org/10.5061/dryad.1597g

Lundelius, E.L., Jr., 1967. Late Pleistocene and Holocene faunal history of central Texas. In: Martin, P.S., Wright, H.E., Jr., (Eds.), *Pleistocene Extinctions, the Search for a Cause*. Yale University Press, New Haven, pp. 287–319.

Lyons, S.K., 2003. A quantitative assessment of the range shifts of Pleistocene mammals. *Journal of Mammalogy* 84, 385–402.

Lyons, S.K., 2005. A quantitative model for assessing community dynamics of Pleistocene mammals. *The American Naturalist* 165, E168–E185.

Lyons, S. K., Smith, F.A., Brown, J.H., 2004. Of mice, mastodons and men: human-mediated extinctions on four continents. *Evolutionary Ecology Research* 6, 339–358.

Macêdo, R.H., Mares, M.A., 1988. *Neotoma albigula*. *Mammalian Species* 31, 1–7.

Malhi, Y., Doughty, C.E., Galetti, M., Smith, F.A., Svenning, J.C., Terborgh, J.W., 2016. Megafauna and ecosystem function from the Pleistocene to the Anthropocene. *Proceedings of the National Academy of Sciences* 113, 838–846.

Martin, P.S., 1967. Prehistoric overkill. In: Martin, P.S., Wright, H.E., Jr. (Eds.), *Pleistocene Extinctions, the Search for a Cause*. Yale University Press, New Haven, pp. 75–120.

Martin, P.S., Klein, R.G., 1989. *Quaternary Extinctions: A Prehistoric Revolution*. University of Arizona Press, Tucson, AZ.

Martin, P.S., Steadman, D.W., 1999. Prehistoric extinctions on islands and continents. In: MacPhee, R.D.S. (Ed.), *Extinctions in Near Time*. Springer, Boston, MA, pp. 17–55.

Martin, R.A., 1990. Estimating body mass and correlated variables in extinct mammals: travels in the fourth dimension. In: Damuth, J., MacFadden, B.J. (Eds.), *Body Size in Mammalian Paleobiology*. Cambridge University Press, Cambridge, UK, pp. 49–68.

Mayr, E., 1956. Geographical character gradients and climatic adaptation. *Evolution* 10, 105–108.

McLister, J.D., Sorensen, J.S., Dearing, M.D., 2004. Effects of consumption of juniper (*Juniperus monosperma*) on cost of thermoregulation in the woodrats *Neotoma albigula* and *Neotoma stephensi* at different acclimation temperatures. *Physiological and Biochemical Zoology* 77, 305–312.

M'Closkey, R.T., 1976. Community structure in sympatric rodents. *Ecology* 57, 728–739.

McNab, B.K., 1980. Food habits, energetics, and the population biology of mammals. *The American Naturalist* 116, 106–124.

Millien, V., Lyons, S.K., Olson, L., Smith, F.A., Wilson, A.B., Yom-Tov, Y., 2006. Ecotypic variation in the context of global climate change: revisiting the rules. *Ecology Letters* 9, 853–869.

Mooney, H.A., Bullock, S.H., Ehleringer, J.R., 1989. Carbon isotope ratios of plants of a tropical dry forest in Mexico. *Functional Ecology* 3, 137–142.

Mooney, H., Troughton, J.H., Berry, J.A., 1974. Arid climates and photosynthetic systems. *Annual Report, Department of Plant Biology, Carnegie Institution* 73, 793–805.

Murray, I.W., Smith, F.A., 2012. Estimating the influence of the thermal environment on activity patterns of the desert woodrat (*Neotoma lepida*) using temperature chronologies. *Canadian Journal of Zoology* 90, 117–1180.

Neotoma Paleoecology Database. 2015. http://www.neotomadb.org/

Newsome, S.D., Martinez del Rio, C., Bearhop, S., Phillips, D.L., 2007. A niche for isotope ecology. *Frontiers in Ecology and the Environment* 5, 429–436.

Nordt, L.C., Boutton, T.W., Hallmark, C.T., Waters, M.R., 1994. Late Quaternary vegetation and climate changes in central Texas based on the isotopic composition of organic carbon. *Quaternary Research* 41, 109–120.

Olsen, R.W., 1976. Water: a limiting factor for a population of wood rats. *The Southwestern Naturalist* 21, 391–398.

Orr, T.J., Newsome, S.D., Wolf, B.O., 2015. Cacti supply limited nutrients to a desert rodent community. *Oecologia* 178, 1045–1062.

Owen-Smith, R.N., 1992. *Megaherbivores: The Influence of Very Large Body Size on Ecology*. Cambridge University Press, Cambridge, UK.

Parnell, A., Jackson, A., 2013. siar: stable isotope Analysis in R. *R package version* 4.2.2. https://CRAN.R-project.org/package=siar

Parsons, E.W.R., Maron, J.L., Martin, T.E., 2013. Elk herbivory alters small mammal assemblages in high-elevation drainages. *Journal of Animal Ecology* 82, 459–467.

Peters, R.H., 1983. *The Ecological Implications of Body Size*. Cambridge University Press, Cambridge, UK.

Prentice, I.C., Bartlein, P.J., Webb, T., III, 1991. Vegetation and climate change in eastern North America since the Last Glacial Maximum. *Ecology* 72, 2038–2056.

Rainey, D.G., 1956. Eastern woodrat, *Neotoma floridana*: life history and ecology. *University of Kansas Publications, Museum of Natural History* 8, 536–646.

Randolph, J.C., Cameron, G.N., Wrazen, J.A., 1991. Dietary choice of a generalist grassland herbivore, *Sigmodon hispidus*. *Journal of Mammalogy* 72: 300–313.

Raun, G.G., 1966. A population of woodrats (*Neotoma micropus*) in southern Texas. *Texas Memorial Museum Bulletin* 11, 1–62.

R Core Team, 2019. R: a language and environment for statistical computing. *R Foundation for Statistical Computing, Vienna, Austria*. https://www.Rproject.org/

Ripple, W.J., Newsome, T.M., Wolf, C., Dirzo, R., Everatt, K.T., Galetti, M., Hayward, M.W., et al., 2015. Collapse of the world's largest herbivores. *Science Advances* 1, e1400103. https://doi.org/10.1126/sciadv.1400103

RStudio Team, 2019. *RStudio: Integrated Development for R*. RStudio Inc. Boston, MA. http://www.rstudio.com/

Rule, S., Brook, B.W., Haberle, S.G., Turney, C.S., Kershaw, A.P., Johnson, C.N., 2012. The aftermath of megafaunal extinction: ecosystem transformation in Pleistocene Australia. *Science* 335, 1483–1486.

Sagebiel, J.C., 2010, Late Pleistocene Fauna from Zesch Cave, Mason County, Texas. *Quaternary International* 217, 159–174.

Schmidly, D.J., Bradley, R.D., 2016. *The Mammals of Texas*. University of Texas Press, Austin, Texas.

Seersholm, F.V., Werndly, D.J., Grealy, A., Johnson, T., Keenan Early, E.M., Lundelius, E.L., Jr., Winsborough, B., et al., 2020. Rapid range shifts and megafaunal extinctions associated with late Pleistocene climate change. *Nature Communications* 11, 2770. https://doi.org/10.1038/s41467-020-16502-3

Sharp, Z., 2017. *Principles of Stable Isotope Geochemistry, 2nd Edition*. University of New Mexico, Digital Repository. https://doi.org/10.5072/FK2GB24S9F

Smiley, T.M., Cotton, J.M., Badgley, C., Cerling, T.E., 2016. Small-mammal isotope ecology tracks climate and vegetation gradients across western North America. *Oikos* 125, 1100–1109.

Smith, F.A., 1995a. Scaling of digestive efficiency with body mass in *Neotoma*. *Functional Ecology* 9, 299–305.

Smith, F.A., 1995b. Den characteristics and survivorship of woodrats (*Neotoma lepida*) in the eastern Mojave Desert. *Southwestern Naturalist* 41, 366–372.

Smith, F.A., 2008. Body size, energetics, and evolution. In: Jorgensen, S.E., Fath, B.D. (Eds.), *Encyclopedia of Ecology*. Elsevier, Amsterdam, pp. 477–482.

Smith, F.A., Betancourt, J.L., 1998. Response of bushy-tailed woodrats (*Neotoma cinerea*) to late Quaternary climatic change in the Colorado Plateau. *Quaternary Research* 50, 1–11.

Smith, F.A., Betancourt, J.L., 2003. The effect of Holocene temperature fluctuations on the evolution and ecology of *Neotoma* (woodrats) in Idaho and northwestern Utah. *Quaternary Research* 59, 160–171.

Smith, F.A., Betancourt, J.L., Brown, J.H., 1995. Evolution of body size in the woodrat over the past 25,000 years of climate change. *Science* 270, 2012–2014.

Smith, F.A., Browning, H., Shepherd, U.L., 1998. The influence of climate change on the body mass of woodrats *Neotoma* in an arid region of New Mexico, USA. *Ecography* 21, 140–148.

Smith, F.A., Doughty, C.E., Malhi, Y., Svenning, J.C., Terborgh, J., 2016a. Megafauna in the Earth system. *Ecography* 39, 99–108.

Smith, F.A., Elliott Smith, R.E., Lyons, S.K., Payne, J.L., 2018. Body size downgrading of mammals over the late Quaternary. *Science* 360, 310–313.

Smith, F.A., Tomé, C.P., Elliott Smith, E.A., Lyons, S.K., Newsome, S.D.,

Stafford, T.W., 2016b. Unraveling the consequences of the terminal Pleistocene megafauna extinction on mammal community assembly. *Ecography* 39, 223–239.

Spencer, D.A., Spencer, A.L., 1941. Food habits of the white-throated wood rat in Arizona. *Journal of Mammalogy* 22, 280–284.

Stanley, S.M., 1973. An explanation for Cope's rule. *Evolution* 27, 1–26.

Stenseth, N.C., Mysterud, A., Ottersen, G., Hurrell, J.W., Chan, K.S., Lima, M., 2002. Ecological effects of climate fluctuations. *Science* 297, 1292–1296.

Stock, B.C., Semmens, B.X., 2016. *MixSIAR GUI user Manual. Version 3.1*. https://github.com/brianstock/MixSIAR

Sutton, B.G., Ting, I.P., Troughton, J.H., 1976. Seasonal effects on carbon isotope composition of cactus in a desert environment. *Nature* 26, 42–43.

Terry, R.C., 2018. Isotopic niche variation from the Holocene to today reveals minimal partitioning and individualistic dynamics among four sympatric desert mice. *Journal of Animal Ecology* 87, 173–186.

Terry, R.C., Guerre, M.E., Taylor, D.S., 2017. How specialized is a diet specialist? Niche flexibility and local persistence through time of the chisel-toothed kangaroo rat. *Functional Ecology* 31, 1921–1932.

Thies, M., Caire, W., 1990. Association of *Neotoma micropus* nests with various plant species in southwestern Oklahoma. *The Southwestern Naturalist* 35, 80–82.

Tomé, C.P., Elliott Smith, E.A., Lyons, S.K., Newsome, S.D., Smith, F.A., 2020a. Changes in the diet and body size of a small herbivorous mammal (hispid cotton rat, *Sigmodon hispidus*) following the late Pleistocene megafauna extinction. *Ecography* 43, 604–619.

Tomé, C.P., Whiteman-Jennings, W., Smith, F.A. 2020b. The relationship between molar morphology and ecology within *Neotoma*. *Journal of Mammalogy* 101, 1711–1726.

Toomey, R.S., III., 1993. *Late Pleistocene and Holocene faunal and environmental changes at Hall's Cave, Kerr County, Texas*. PhD dissertation, University of Texas, Austin, Texas, USA, 560 pp.

Toomey, R.S., III., Blum, M.D., Valastro Jr, S., 1993. Late Quaternary climates and environments of the Edwards Plateau, Texas. *Global Planetary Change* 7, 299–320.

Tóth, A.B., Lyons, S.K., Barr, W.A., Behrensmeyer, A.K., Blois, J.L., Bobe, R., Matt Davis, M., et al., 2019. Reorganization of surviving mammal communities after the end-Pleistocene megafaunal extinction. *Science* 365, 1305–1308.

Verts, B.J., Carraway, L.N., 2002. *Neotoma lepida*. *Mammalian Species* 699, 1–12.

Vorhies, C.T., Taylor, W.P., 1940. Life history and ecology of the white-throated wood rat, *Neotoma albigula* Hartley, in relation to grazing in Arizona. *College of Agriculture, University of Arizona, Tucson, AZ, Technical Bulletin* 86, 455–528.

Walsh, R.E., Aprigio Assis, A.P., Patton, J.L., Marroig, G., Dawson, T.E., Lacey, E.A., 2016. Morphological and dietary responses of chipmunks to a century of climate change. *Global Change Biology* 22, 3233–3252.

West, J.B., Bowen, G.J., Cerling, T.E., Ehleringer, J.R., 2006. Stable isotopes as one of nature's ecological recorders. *Trends in Ecology & Evolution* 21, 408–414.

Wiley, R.W., 1980. *Neotoma floridana*. *Mammalian Species* 139, 1–7.

**SUPPLEMENTARY MATERIAL TABLE AND FIGURE CAPTIONS**

## TABLES

**Table S1.** Results for differences in the distributions (Two-Sample T-Test) and variance (Levene Test) of *Neotoma* mass and diet ($\delta^{13}C$ and $\delta^{15}N$) between specimens from Zesch Cave (Collection ID 40685) versus Hall's Cave (Collection ID 41229) within the time interval 22,400-15,800 cal yr BP.

**Table S2.** Measurements of first upper and lower molars of modern *Neotoma* from the Bell Museum of Natural History (MMNH) and the Museum of Southwestern Biology (MSB). Mean lengths of upper left (ULM1) and right (URM1), lower left (LLM1) and right (LRM1) first molars are given with standard error (SE).

**Table S3.** Results for changes in the distributions and variance of *Neotoma* mass and diet ($\delta^{13}C$ and $\delta^{15}N$) for pre- (22,400-12,700 cal yr BP) and post-extinction (12,700-0 cal yr BP) time bins. * Welsh Two-Sample T-Test used to account for unequal variances between groups.

**Table S4.** Tukey Honest Significant Differences (Diff.) on ANOVA of mass ($p<0.05$, df=14/451), $\delta^{13}C$ ($p<0.001$, df=14/291), and $\delta^{15}N$ ($p<0.01$, df=14/291) across all time interval. Significant p-values are bolded.

**Table S5.** Results of AIC and multiple linear models comparing mass and diet ($\delta^{13}C$ and $\delta^{15}N$) to climate and community metrics (richness, turnover, similarity to modern). Models were run on maximum and median mass due to the potential for multiple species of *Neotoma.* Precipitation (mm) (Precip), maximum and minimum temperature ($^{o}C$) (Max_Temp and Min_Temp) were extracted from the CCM3 (Lorenz et al. 2016a,b). Significant p-values are bolded.

**Table S6.** Results of linear models comparing mass and diet in *Neotoma*. Significant p-values are bolded.

**Table S7.** Results of sliding window linear models for maximum and median mass (g) of *Neotoma* against climate (precipitation and temperature) and community (richness, turnover and similarity to modern). Turnover here is the calculated Sorenson as similarity to the youngest time interval. Each window included 6 time intervals as given in cal yr BP in Table 1. Rows with significant p-values are bolded.

**FIGURES**

**Figure S1. Changes in *Neotoma* across the megafaunal extinction event.** Boxplots show mean and interquartile ranges for A) mass, B) $\delta^{13}C$ and C) $\delta^{15}N$ distributions of the *Neotoma*, before (pre-) and after (post-) the megafaunal extinction.

**Figure S2. Bayesian standard ellipse area for *Neotoma* through time.** Bayesian standard ellipse area ($SEA_B$) from $\delta^{13}C$ and $\delta^{15}N$ bone collagen values for *Neotoma* across 15 time intervals (as midpoint), 50%, 90% and 95% credible intervals (gray boxes) and mean values (black dots).

**SUPPLEMENTARY MATERIAL TABLE S1**

| | Levene-Test | | | Two Sample T-Test | | |
|---|---|---|---|---|---|---|
| | F | df | p-value | t | df | p-value |
| Mass | 0.78 | 1/21 | 0.3881 | 1.38 | 21 | 0.182 |
| $\delta^{13}C$ | 3.75 | 1/3 | 0.148 | 1.01 | 3 | 0.3882 |
| $\delta^{15}N$ | 1.11 | 1/3 | 0.370 | 0.87 | 3 | 0.450 |

**SUPPLEMENTARY MATERIAL TABLE S2**

| Museum ID | Specimen ID | ULM1 ± SE | URM1 ± SE | LLM1 ± SE | LRM1 ± SE |
|---|---|---|---|---|---|
| MMNH | 10254 | 3.42 ± 0.02 | 3.41 ± 0.01 | 3.19 ± 0.00 | 3.16 ± 0.00 |
| MMNH | 11399 | 3.29 ± 0.01 | 3.17 ± 0.00 | 3.05 ± 0.01 | 3.11 ± 0.01 |
| MMNH | 11400 | 3.57 ± 0.01 | 3.55 ± 0.02 | 3.40 ± 0.02 | 3.32 ± 0.00 |
| MMNH | 11401 | 3.64 ± 0.03 | 3.68 ± 0.00 | 3.24 ± 0.01 | 3.26 ± 0.01 |
| MMNH | 11403 | 3.47 ± 0.01 | 3.6 ± 0.00 | 3.38 ± 0.01 | 3.30 ± 0.00 |
| MMNH | 11404 | 3.34 ± 0.03 | 3.36 ± 0.03 | 3.09 ± 0.01 | 3.12 ± 0.00 |
| MMNH | 12621 | 3.41 ± 0.03 | 3.39 ± 0.02 | 3.19 ± 0.04 | 3.18 ± 0.01 |
| MMNH | 12622 | 3.21 ± 0.01 | 3.26 ± 0.01 | 3.37 ± 0.04 | 3.41 ± 0.02 |
| MMNH | 12623 | 3.28 ± 0.02 | 3.26 ± 0.01 | 3.19 ± 0.00 | 3.28 ± 0.02 |
| MMNH | 12627 | 3.28 ± 0.02 | 3.25 ± 0.01 | 3.07 ± 0.01 | 3.07 ± 0.00 |
| MMNH | 12628 | 3.45 ± 0.01 | 3.39 ± 0.01 | 3.48 ± 0.00 | 3.42 ± 0.01 |
| MMNH | 12629 | 3.69 ± 0.01 | 3.52 ± 0.03 | 3.81 ± 0.01 | 3.63 ± 0.03 |
| MSB | 109867 | 3.12 ± 0.02 | 3.13 ± 0.01 | 2.86 ± 0.01 | 2.77 ± 0.02 |
| MSB | 109868 | 3.25 ± 0.00 | 3.17 ± 0.00 | 2.82 ± 0.02 | 2.82 ± 0.00 |
| MSB | 109963 | 2.88 ± 0.00 | 2.88 ± 0.00 | 2.62 ± 0.01 | 2.66 ± 0.01 |
| MSB | 109964 | 3.02 ± 0.00 | 2.94 ± 0.01 | 2.75 ± 0.02 | 2.74 ± 0.01 |
| MSB | 109998 | 3.28 ± 0.01 | 3.19 ± 0.00 | 3.07 ± 0.01 | 3.11 ± 0.01 |
| MSB | 109999 | 2.86 ± 0.00 | 2.89 ± 0.01 | 2.88 ± 0.01 | 2.85 ± 0.00 |
| MSB | 121289 | 3.04 ± 0.00 | 3.01 ± 0.01 | 2.92 ± 0.01 | 2.87 ± 0.00 |
| MSB | 121308 | 3.23 ± 0.00 | 3.17 ± 0.03 | 3.15 ± 0.01 | 3.15 ± 0.01 |
| MSB | 121332 | 3.05 ± 0.01 | 3.03 ± 0.00 | 2.92 ± 0.01 | 2.92 ± 0.00 |
| MSB | 121401 | 3.21 ± 0.01 | 3.11 ± 0.02 | 3.05 ± 0.01 | 3.08 ± 0.02 |

**SUPPLEMENTARY MATERIAL TABLE S3**

| | F-Test | | | Bartlett Test | | | Two Sample T-Test | | | Wilcoxon Rank Sum Test | |
|---|---|---|---|---|---|---|---|---|---|---|---|
| | F | df | p-value | K-squared | df | p-value | t | df | p-value | W | p-value |
| Mass | 1.40 | 78/350 | 0.044 | 3.88 | 1 | 0.049 | 1.77 | 104.46 | 0.07895* | 15693.0 | 0.067 |
| $\delta^{13}C$ | 0.42 | 33/271 | 0.004 | 8.73 | 1 | 0.003 | -3.10 | 54.92 | 0.003087* | 3506.0 | 0.022 |
| $\delta^{15}N$ | 1.44 | 33/271 | 0.128 | 2.10 | 1 | 0.147 | -4.28 | 304.00 | 2.554E-05 | 2530.5 | 1.674E-05 |

**SUPPLEMENTARY MATERIAL TABLE S4**

| | | Mass (g) | | $\delta^{13}C$ (‰) | | $\delta^{15}N$ (‰) | |
|---|---|---|---|---|---|---|---|
| Upper Mid-age (cal BP) | Lower Mid-age (cal BP) | Diff. | p-value | Diff. | p-value | Diff. | p-value |
| 2300 | 750 | 15.8 | 1.000 | -1.6 | 0.912 | -0.2 | 1.000 |
| 4250 | 750 | 39.0 | 0.441 | 0.0 | 1.000 | -0.1 | 1.000 |
| 5750 | 750 | 34.5 | 0.778 | 0.0 | 1.000 | -0.4 | 1.000 |
| 6250 | 750 | 27.2 | 0.980 | 0.1 | 1.000 | 0.0 | 1.000 |
| 6550 | 750 | 21.6 | 0.999 | -0.8 | 1.000 | -0.7 | 0.998 |
| 7200 | 750 | 18.8 | 0.998 | 0.9 | 0.998 | 0.0 | 1.000 |
| 8050 | 750 | 39.6 | 0.685 | -0.4 | 1.000 | -0.1 | 1.000 |
| 8700 | 750 | 38.6 | 0.649 | 0.3 | 1.000 | 0.6 | 0.998 |
| 9200 | 750 | 50.9 | 0.452 | -0.5 | 1.000 | 0.6 | 1.000 |
| 9700 | 750 | 49.4 | 0.248 | 0.0 | 1.000 | 0.3 | 1.000 |
| 10500 | 750 | 46.3 | 0.256 | -1.6 | 0.792 | 0.0 | 1.000 |
| 11850 | 750 | 35.1 | 0.650 | -1.4 | 0.945 | 0.1 | 1.000 |
| 14250 | 750 | 39.9 | 0.418 | -1.2 | 0.983 | -0.9 | 0.899 |
| 19100 | 750 | 56.5 | 0.079 | -1.7 | 0.982 | -1.7 | 0.554 |
| 4250 | 2300 | 23.2 | 0.515 | 1.6 | 0.499 | 0.1 | 1.000 |
| 5750 | 2300 | 18.6 | 0.961 | 1.6 | 0.699 | -0.2 | 1.000 |
| 6250 | 2300 | 11.3 | 1.000 | 1.7 | 0.855 | 0.2 | 1.000 |
| 6550 | 2300 | 5.7 | 1.000 | 0.8 | 1.000 | -0.5 | 1.000 |
| 7200 | 2300 | 3.0 | 1.000 | 2.5 | **0.022** | 0.2 | 1.000 |
| 8050 | 2300 | 23.8 | 0.913 | 1.2 | 0.953 | 0.1 | 1.000 |
| 8700 | 2300 | 22.7 | 0.877 | 1.9 | 0.390 | 0.8 | 0.891 |
| 9200 | 2300 | 35.1 | 0.709 | 1.1 | 0.996 | 0.8 | 0.988 |
| 9700 | 2300 | 33.5 | 0.339 | 1.6 | 0.699 | 0.5 | 0.997 |

| | | | | | | | |
|---|---|---|---|---|---|---|---|
| 10500 | 2300 | 30.5 | 0.297 | 0.0 | 1.000 | 0.2 | 1.000 |
| 11850 | 2300 | 19.2 | 0.838 | 0.2 | 1.000 | 0.3 | 1.000 |
| 14250 | 2300 | 24.0 | 0.491 | 0.4 | 1.000 | -0.7 | 0.951 |
| 19100 | 2300 | 40.7 | 0.068 | -0.1 | 1.000 | -1.5 | 0.650 |
| 5750 | 4250 | -4.6 | 1.000 | 0.0 | 1.000 | -0.3 | 0.999 |
| 6250 | 4250 | -11.9 | 1.000 | 0.2 | 1.000 | 0.1 | 1.000 |
| 6550 | 4250 | -17.5 | 0.997 | -0.8 | 0.999 | -0.6 | 0.992 |
| 7200 | 4250 | -20.2 | 0.779 | 0.9 | 0.825 | 0.1 | 1.000 |
| 8050 | 4250 | 0.6 | 1.000 | -0.4 | 1.000 | 0.0 | 1.000 |
| 8700 | 4250 | -0.5 | 1.000 | 0.3 | 1.000 | 0.7 | 0.726 |
| 9200 | 4250 | 11.9 | 1.000 | -0.4 | 1.000 | 0.7 | 0.986 |
| 9700 | 4250 | 10.3 | 1.000 | 0.0 | 1.000 | 0.4 | 0.994 |
| 10500 | 4250 | 7.3 | 1.000 | -1.6 | 0.072 | 0.1 | 1.000 |
| 11850 | 4250 | -4.0 | 1.000 | -1.4 | 0.473 | 0.2 | 1.000 |
| 14250 | 4250 | 0.8 | 1.000 | -1.1 | 0.617 | -0.8 | 0.377 |
| 19100 | 4250 | 17.5 | 0.965 | -1.7 | 0.938 | -1.6 | 0.355 |
| 6250 | 5750 | -7.3 | 1.000 | 0.1 | 1.000 | 0.4 | 1.000 |
| 6550 | 5750 | -12.9 | 1.000 | -0.8 | 0.999 | -0.2 | 1.000 |
| 7200 | 5750 | -15.6 | 0.993 | 0.9 | 0.975 | 0.4 | 0.998 |
| 8050 | 5750 | 5.2 | 1.000 | -0.4 | 1.000 | 0.4 | 1.000 |
| 8700 | 5750 | 4.1 | 1.000 | 0.3 | 1.000 | 1.0 | 0.351 |
| 9200 | 5750 | 16.5 | 1.000 | -0.5 | 1.000 | 1.0 | 0.822 |
| 9700 | 5750 | 14.9 | 0.999 | 0.0 | 1.000 | 0.8 | 0.832 |
| 10500 | 5750 | 11.9 | 1.000 | -1.6 | 0.332 | 0.5 | 0.994 |
| 11850 | 5750 | 0.6 | 1.000 | -1.4 | 0.733 | 0.6 | 0.986 |
| 14250 | 5750 | 5.4 | 1.000 | -1.2 | 0.862 | -0.4 | 0.998 |
| 19100 | 5750 | 22.1 | 0.933 | -1.7 | 0.956 | -1.2 | 0.839 |
| 6550 | 6250 | -5.6 | 1.000 | -1.0 | 1.000 | -0.6 | 0.999 |
| 7200 | 6250 | -8.3 | 1.000 | 0.8 | 1.000 | 0.0 | 1.000 |
| 8050 | 6250 | 12.5 | 1.000 | -0.5 | 1.000 | 0.0 | 1.000 |

| | | | | | | | |
|---|---|---|---|---|---|---|---|
| 8700 | 6250 | 11.4 | 1.000 | 0.2 | 1.000 | 0.6 | 0.995 |
| 9200 | 6250 | 23.8 | 0.994 | -0.6 | 1.000 | 0.6 | 1.000 |
| 9700 | 6250 | 22.2 | 0.981 | -0.1 | 1.000 | 0.4 | 1.000 |
| 10500 | 6250 | 19.1 | 0.990 | -1.7 | 0.692 | 0.1 | 1.000 |
| 11850 | 6250 | 7.9 | 1.000 | -1.5 | 0.898 | 0.2 | 1.000 |
| 14250 | 6250 | 12.7 | 1.000 | -1.3 | 0.961 | -0.8 | 0.931 |
| 19100 | 6250 | 29.4 | 0.816 | -1.8 | 0.968 | -1.6 | 0.601 |
| 7200 | 6550 | -2.7 | 1.000 | 1.7 | 0.561 | 0.6 | 0.983 |
| 8050 | 6550 | 18.1 | 0.999 | 0.4 | 1.000 | 0.6 | 0.995 |
| 8700 | 6550 | 17.0 | 0.999 | 1.1 | 0.986 | 1.3 | 0.330 |
| 9200 | 6550 | 29.4 | 0.976 | 0.4 | 1.000 | 1.2 | 0.716 |
| 9700 | 6550 | 27.8 | 0.939 | 0.8 | 0.999 | 1.0 | 0.742 |
| 10500 | 6550 | 24.7 | 0.959 | -0.8 | 0.999 | 0.7 | 0.970 |
| 11850 | 6550 | 13.5 | 1.000 | -0.6 | 1.000 | 0.8 | 0.948 |
| 14250 | 6550 | 18.3 | 0.996 | -0.3 | 1.000 | -0.2 | 1.000 |
| 19100 | 6550 | 34.9 | 0.706 | -0.9 | 1.000 | -1.0 | 0.980 |
| 8050 | 7200 | 20.8 | 0.974 | -1.3 | 0.626 | 0.0 | 1.000 |
| 8700 | 7200 | 19.7 | 0.963 | -0.6 | 0.999 | 0.6 | 0.919 |
| 9200 | 7200 | 32.1 | 0.834 | -1.4 | 0.924 | 0.6 | 0.997 |
| 9700 | 7200 | 30.5 | 0.536 | -0.9 | 0.975 | 0.4 | 1.000 |
| 10500 | 7200 | 27.5 | 0.518 | -2.5 | **0.000** | 0.0 | 1.000 |
| 11850 | 7200 | 16.2 | 0.962 | -2.3 | **0.011** | 0.1 | 1.000 |
| 14250 | 7200 | 21.0 | 0.753 | -2.1 | **0.014** | -0.9 | 0.369 |
| 19100 | 7200 | 37.7 | 0.154 | -2.6 | 0.400 | -1.6 | 0.315 |
| 8700 | 8050 | -1.1 | 1.000 | 0.7 | 0.999 | 0.7 | 0.926 |
| 9200 | 8050 | 11.3 | 1.000 | -0.1 | 1.000 | 0.6 | 0.996 |
| 9700 | 8050 | 9.7 | 1.000 | 0.4 | 1.000 | 0.4 | 0.999 |
| 10500 | 8050 | 6.7 | 1.000 | -1.2 | 0.779 | 0.1 | 1.000 |
| 11850 | 8050 | -4.6 | 1.000 | -1.0 | 0.974 | 0.2 | 1.000 |
| 14250 | 8050 | 0.2 | 1.000 | -0.7 | 0.996 | -0.8 | 0.637 |

| | | | | | | | |
|---|---|---|---|---|---|---|---|
| 19100 | 8050 | 16.9 | 0.998 | -1.3 | 0.996 | -1.6 | 0.415 |
| 9200 | 8700 | 12.4 | 1.000 | -0.8 | 1.000 | 0.0 | 1.000 |
| 9700 | 8700 | 10.8 | 1.000 | -0.3 | 1.000 | -0.3 | 1.000 |
| 10500 | 8700 | 7.7 | 1.000 | -1.9 | 0.089 | -0.6 | 0.945 |
| 11850 | 8700 | -3.5 | 1.000 | -1.7 | 0.386 | -0.5 | 0.996 |
| 14250 | 8700 | 1.3 | 1.000 | -1.4 | 0.521 | -1.5 | **0.005** |
| 19100 | 8700 | 18.0 | 0.992 | -2.0 | 0.858 | -2.3 | **0.030** |
| 9700 | 9200 | -1.6 | 1.000 | 0.5 | 1.000 | -0.2 | 1.000 |
| 10500 | 9200 | -4.6 | 1.000 | -1.1 | 0.986 | -0.5 | 0.999 |
| 11850 | 9200 | -15.9 | 1.000 | -0.9 | 0.999 | -0.4 | 1.000 |
| 14250 | 9200 | -11.1 | 1.000 | -0.7 | 1.000 | -1.4 | 0.186 |
| 19100 | 9200 | 5.6 | 1.000 | -1.2 | 0.999 | -2.2 | 0.114 |
| 10500 | 9700 | -3.1 | 1.000 | -1.6 | 0.332 | -0.3 | 1.000 |
| 11850 | 9700 | -14.3 | 0.997 | -1.4 | 0.733 | -0.2 | 1.000 |
| 14250 | 9700 | -9.5 | 1.000 | -1.2 | 0.862 | -1.2 | 0.080 |
| 19100 | 9700 | 7.2 | 1.000 | -1.7 | 0.956 | -2.0 | 0.109 |
| 11850 | 10500 | -11.2 | 0.999 | 0.2 | 1.000 | 0.1 | 1.000 |
| 14250 | 10500 | -6.4 | 1.000 | 0.4 | 1.000 | -0.9 | 0.274 |
| 19100 | 10500 | 10.2 | 1.000 | -0.1 | 1.000 | -1.7 | 0.272 |
| 14250 | 11850 | 4.8 | 1.000 | 0.2 | 1.000 | -1.0 | 0.306 |
| 19100 | 11850 | 21.5 | 0.864 | -0.3 | 1.000 | -1.8 | 0.244 |
| 19100 | 14250 | 16.7 | 0.980 | -0.5 | 1.000 | -0.8 | 0.994 |

**SUPPLEMENTARY MATERIAL TABLE S5**

| Climate Models | | | | | | | | |
|---|---|---|---|---|---|---|---|---|
| | **Best model** | | **Slope(s)** | **AIC** | **F-statistic** | **df** | **p-value** | **Adjusted $r^2$** |
| Maximum Mass | Precip | *pos.* | *0.65* | 101.87 | 15.88 | 1/13 | **0.002** | **0.52** |
| Median Mass | Max_Temp | *neg.* | *4.39* | 82.07 | 4.384 | 1/13 | 0.056 | 0.19 |
| Maximum $\delta^{13}C$ | Min_Temp | *pos.* | *1.24* | 22.68 | 8.976 | 1/13 | **0.010** | **0.36** |
| Mean $\delta^{13}C$ | Precip | *neg.* | *0.01* | 10.34 | 7.679 | 1/13 | **0.016** | **0.32** |
| Minimum $\delta^{13}C$ | Max_Temp | *neg.* | *0.23* | -6.32 | 4.372 | 1/13 | 0.057 | 0.19 |
| Maximum $\delta^{15}N$ | Max_Temp + Min_Temp + Precip | *neg., pos., pos.* | *0.02, 1.56, 3.19* | -7.86 | 9.222 | 3/11 | **0.002** | **0.64** |
| Mean $\delta^{15}N$ | Max_Temp + Min_Temp | *neg., pos.* | *0.6, 1.19* | -32.44 | 17.97 | 2/12 | **2.462E-04** | **0.71** |
| Minimum $\delta^{15}N$ | Min_Temp | *pos.* | *0.22* | -28.14 | 8.64 | 1/13 | **0.012** | **0.35** |

| Community Models | | | | | | | | |
|---|---|---|---|---|---|---|---|---|
| | **Best model** | | **Slope(s)** | **AIC** | **F-statistic** | **df** | **p-value** | **Adjusted $r^2$** |
| Maximum Mass | Richness + Turnover + Similarity | *neg., neg., neg.* | *2.35, 74.85, 382.31* | 87.59 | 23.89 | 3/11 | **4.041E-05** | **0.82** |
| Median Mass | Richness + Turnover + Similarity | *neg., neg., neg.* | *1.02, 66.73, 138.19* | 75.26 | 6.413 | 3/11 | **0.009** | **0.54** |
| Maximum $\delta^{13}C$ | Richness | *neg.* | *0.1* | 26.34 | 4.22 | 1/13 | 0.061 | 0.19 |
| Mean $\delta^{13}C$ | Richness + Turnover | *neg., pos.* | *0.03, 4.18* | 13.56 | 7.2 | 2/12 | **0.008** | **0.48** |
| Minimum $\delta^{13}C$ | Richness + Similarity | *neg., neg.* | *0.06, 7.31* | 10.93 | 6.459 | 2/12 | **0.012** | **0.44** |
| Maximum $\delta^{15}N$ | Turnover | *neg.* | *8.46* | 0.78 | 6.672 | 1/13 | **0.02** | **0.29** |
| Mean $\delta^{15}N$ | Similarity | *pos.* | *1.89* | -18.64 | 5.111 | 1/13 | **0.042** | **0.23** |
| Minimum $\delta^{15}N$ | Similarity | *pos.* | *1.55* | -25.84 | 5.563 | 1/13 | **0.035** | **0.25** |

**SUPPLEMENTARY MATERIAL TABLE S6**

| Variables Compared | F-statistic | df | p-value | Adjusted $r^2$ |
|---|---|---|---|---|
| Mass - $\delta^{13}C$ | 0.21 | 1/129 | 0.649 | -0.01 |
| Mass - $\delta^{15}N$ | 0.05 | 1/129 | 0.827 | -0.01 |
| $\delta^{13}C$ - $\delta^{15}N$ | 57.86 | 1/304 | **3.550E-13** | 0.16 |

## SUPPLEMENTARY MATERIAL TABLE S7

| Maximum Mass | | | | | | | | | | | | | | | | | | |
|---|---|---|---|---|---|---|---|---|---|---|---|---|---|---|---|---|---|---|
| | Precipitation | | | Maximum Temperature | | | Minimum Temperature | | | Richness | | | Turnover | | | Similarity to Modern | | |
| Window (cal yr BP) | p-value | Adjusted $r^2$ | Relation | p-value | Adjusted $r^2$ | Relation | p-value | Adjusted $r^2$ | Relation | p-value | Adjusted $r^2$ | Relation | p-value | Adjusted $r^2$ | Relation | p-value | Adjusted $r^2$ | Relation |
| 6,700-0 | 0.820 | -0.23 | *pos.* | 0.402 | -0.03 | *neg.* | 0.251 | 0.14 | *neg.* | 0.112 | 0.39 | *pos.* | 0.925 | -0.25 | *neg.* | **0.003** | **0.89** | ***neg.*** |
| 7,700-1,500 | 0.229 | 0.17 | *pos.* | 0.867 | -0.24 | *pos.* | 0.842 | -0.24 | *neg.* | 0.155 | 0.29 | *pos.* | 0.971 | -0.25 | *pos.* | 0.052 | 0.57 | *neg.* |
| 8,400-3,100 | 0.196 | 0.22 | *pos.* | 0.347 | 0.03 | *pos.* | 0.254 | 0.13 | *neg.* | 0.717 | -0.20 | *neg.* | 0.123 | 0.36 | *neg.* | 0.114 | 0.38 | *neg.* |
| 9,000-5,400 | 0.520 | -0.11 | *pos.* | 0.484 | -0.09 | *pos.* | 0.729 | -0.21 | *neg.* | 0.395 | -0.02 | *neg.* | 0.273 | 0.11 | *neg.* | 0.825 | -0.23 | *neg.* |
| 9,400-6,100 | 0.981 | -0.25 | *pos.* | 0.858 | -0.24 | *pos.* | 0.548 | -0.13 | *neg.* | 0.565 | -0.14 | *neg.* | 0.458 | -0.07 | *neg.* | 0.565 | -0.14 | *neg.* |
| 10,000-6,400 | 0.400 | -0.02 | *pos.* | 0.938 | -0.25 | *pos.* | **0.026** | **0.69** | ***neg.*** | 0.210 | 0.20 | *pos.* | 0.848 | -0.24 | *neg.* | 0.281 | 0.10 | *neg.* |
| 11,000-6,700 | **0.020** | **0.72** | ***pos.*** | **0.048** | **0.58** | ***neg.*** | 0.074 | 0.49 | *neg.* | **0.014** | **0.77** | ***pos.*** | 0.256 | 0.13 | *neg.* | **0.024** | **0.70** | ***neg.*** |
| 12,700-7,700 | **0.028** | **0.67** | ***pos.*** | 0.122 | 0.36 | *neg.* | 0.100 | 0.41 | *neg.* | **0.026** | **0.69** | ***pos.*** | 0.309 | 0.07 | *neg.* | 0.074 | 0.49 | *neg.* |
| 15,800-8,400 | **0.018** | **0.73** | ***pos.*** | **0.044** | **0.60** | ***neg.*** | **0.033** | **0.65** | ***neg.*** | **0.016** | **0.75** | ***pos.*** | 0.310 | 0.06 | *neg.* | **0.043** | **0.60** | ***neg.*** |
| 22,400-9,000 | **0.008** | **0.82** | ***pos.*** | **0.001** | **0.93** | ***neg.*** | **0.001** | **0.95** | ***neg.*** | 0.092 | 0.44 | *pos.* | 0.291 | 0.09 | *pos.* | **0.011** | **0.80** | ***neg.*** |

| Median Mass | | | | | | | | | | | | | | | | | | |
|---|---|---|---|---|---|---|---|---|---|---|---|---|---|---|---|---|---|---|
| | Precipitation | | | Maximum Temperature | | | Minimum Temperature | | | Richness | | | Turnover | | | Similarity to Modern | | |
| Window (cal yr BP) | p-value | Adjusted r2 | Relation | p-value | Adjusted r2 | Relation | p-value | Adjusted r2 | Relation | p-value | Adjusted r2 | Relation | p-value | Adjusted r2 | Relation | p-value | Adjusted r2 | Relation |
| 6,700-0 | 0.675 | -0.19 | *pos.* | 0.495 | -0.10 | *neg.* | 0.061 | 0.53 | *neg.* | 0.325 | 0.05 | *neg.* | 0.343 | 0.03 | *neg.* | 0.052 | 0.57 | *neg.* |
| 7,700-1,500 | **0.001** | **0.93** | ***pos.*** | 0.939 | -0.25 | *pos.* | 0.465 | -0.08 | *neg.* | 0.417 | -0.04 | *neg.* | 0.327 | 0.05 | *neg.* | 0.329 | 0.04 | *neg.* |
| 8,400-3,100 | **0.041** | **0.61** | ***pos.*** | 0.963 | -0.25 | *neg.* | 0.359 | 0.01 | *neg.* | 0.708 | -0.20 | *neg.* | **0.005** | **0.86** | ***neg.*** | 0.103 | 0.41 | *neg.* |
| 9,000-5,400 | 0.275 | 0.11 | *pos.* | 0.205 | 0.20 | *neg.* | 0.606 | -0.16 | *pos.* | 0.461 | -0.07 | *pos.* | 0.499 | -0.10 | *neg.* | **0.033** | **0.65** | ***neg.*** |
| 9,400-6,100 | **0.021** | **0.72** | ***pos.*** | 0.118 | 0.37 | *neg.* | 0.811 | -0.23 | *pos.* | **0.014** | **0.77** | ***pos.*** | 0.070 | 0.50 | *neg.* | **0.014** | **0.77** | ***neg.*** |
| 10,000-6,400 | **0.017** | **0.74** | ***pos.*** | 0.055 | 0.55 | *neg.* | 0.304 | 0.07 | *neg.* | 0.069 | 0.50 | *pos.* | 0.345 | 0.03 | *neg.* | **0.010** | **0.80** | ***neg.*** |
| 11,000-6,700 | 0.106 | 0.40 | *pos.* | 0.240 | 0.15 | *neg.* | 0.369 | 0.00 | *neg.* | 0.079 | 0.47 | *pos.* | 0.327 | 0.05 | *neg.* | **0.013** | **0.78** | ***neg.*** |
| 12,700-7,700 | 0.863 | -0.24 | *neg.* | 0.508 | -0.10 | *pos.* | 0.515 | -0.11 | *pos.* | 0.918 | -0.25 | *neg.* | 0.872 | -0.24 | *neg.* | 0.917 | -0.25 | *pos.* |
| 15,800-8,400 | 0.240 | 0.15 | *neg.* | 0.185 | 0.24 | *pos.* | 0.240 | 0.15 | *pos.* | 0.310 | 0.07 | *neg.* | 0.983 | -0.25 | *pos.* | 0.223 | 0.18 | *pos.* |
| 22,400-9,000 | 0.576 | -0.14 | *neg.* | 0.905 | -0.24 | *pos.* | 0.949 | -0.25 | *neg.* | 0.316 | 0.06 | *neg.* | 0.422 | -0.04 | *pos.* | 0.631 | -0.17 | *pos.* |

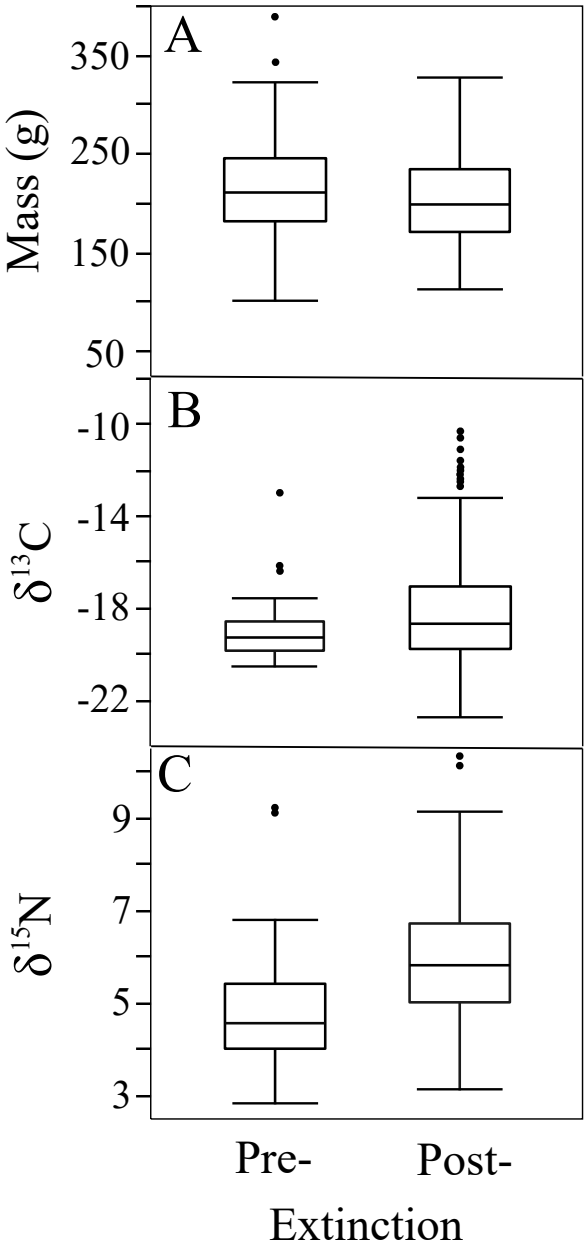


Figure S1. Changes in Neotoma across the megafaunal extinction event. Boxplots show mean and interquartile ranges for A) mass, B) $\delta^{13}C$ and C) $\delta^{15}N$ distributions of the Neotoma, before (pre-) and after (post-) the megafaunal extinction.

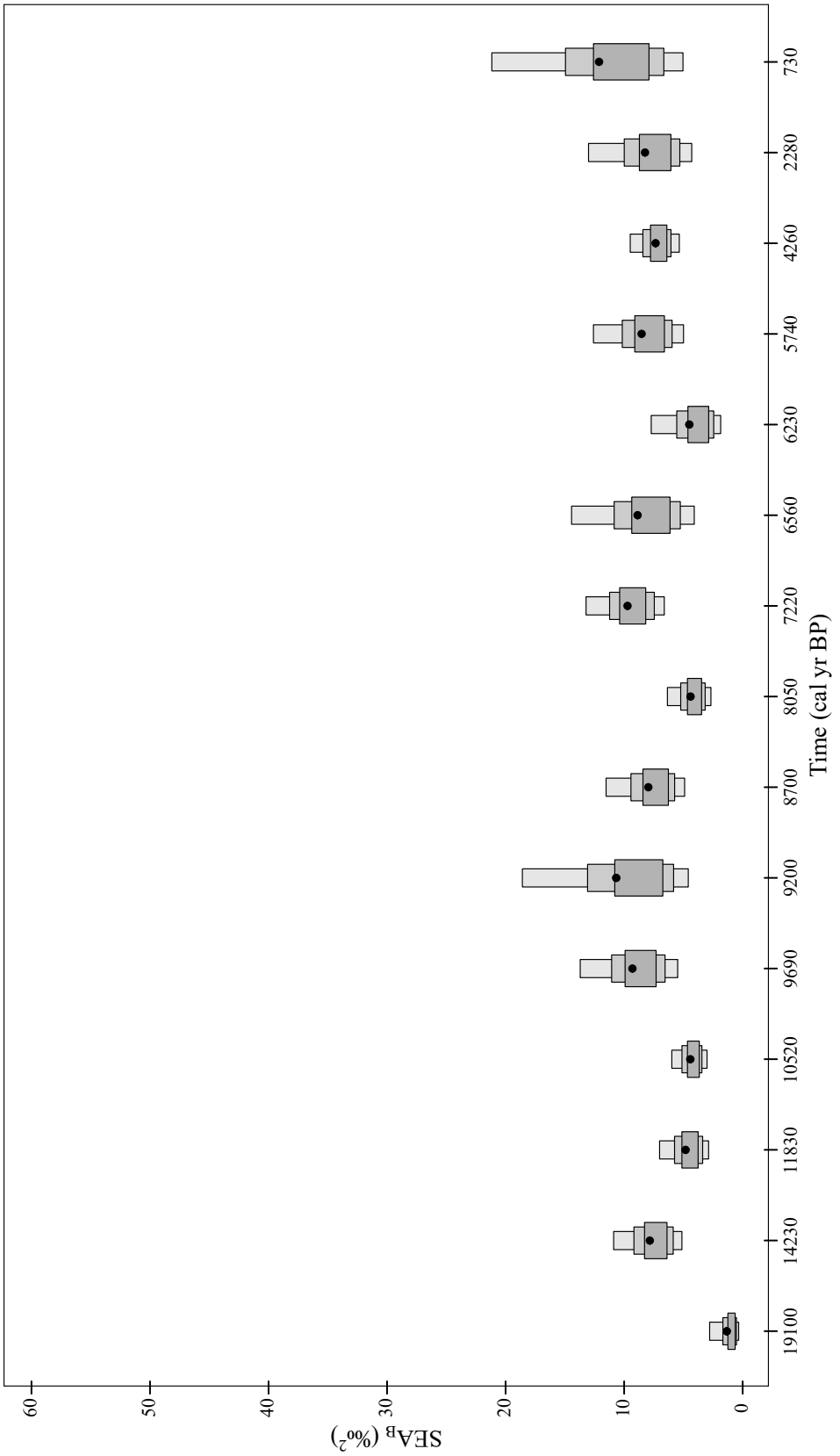


**Figure S2.** Bayesian standard ellipse area for Neotoma through time. Bayesian standard ellipse area ($SEA_B$) from $\delta^{13}C$ and $\delta^{15}N$ bone collagen values for Neotoma across 15 time intervals (as midpoint), 50%, 90% and 95% credible intervals (gray boxes) and mean values (black dots).